# Modelling compressible dense and dilute two-phase flows

Richard Saurel, Ashwin Chinnayya, Quentin Carmouze

# Modelling compressible dense and dilute two-phase flows

Richard Saurel[(1,2)], Ashwin Chinnayya[(3)] and Quentin Carmouze [(2,4)]

[(1)]Aix Marseille Université and IUF, CNRS, Centrale Marseille, M2P2, Marseille, France
[(2)]RS2N, 371 chemin de Gaumin, 83640 Saint-Zacharie, France
[(3)] Institut Pprime, UPR CNRS 3346, ENSMA, Université de Poitiers, 1 avenue Clément Ader, BP 40109, 86961 Futuroscope Chasseneuil Cedex
[(4)] University of Nice, LJAD UMR CNRS 7351, Parc Valrose, 06108 Nice Cedex, France

**Abstract**

Many two-phase flow situations, from engineering science to astrophysics, deal with transition from dense (high concentration of the condensed phase) to dilute concentration (low concentration of the same phase), covering the entire range of volume fractions. Some models are now well accepted at the two limits, but none is able to cover accurately the entire range, in particular regarding waves propagation. In the present work an alternative to the Baer and Nunziato (1986) (BN for short) model, initially designed for dense flows, is built. The corresponding model is hyperbolic and thermodynamically consistent. Contrarily to the BN model that involves 6 wave speeds, the new formulation involves 4 waves only, in agreement with the Marble (1963) model based on pressureless Euler equations for the dispersed phase, a well-accepted model for low particle volume concentrations. In the new model, the presence of pressure in the momentum equation of the particles and consideration of volume fractions in the two phases render the model valid for large particle concentrations. A symmetric version of the new model is derived as well for liquids containing gas bubbles. This model version involves 4 wave speeds as well, but with different wave's speeds. Last, the two sub-models with 4 waves are combined in a unique formulation, valid for the full range of volume fractions. It involves the same 6 wave's speeds as the BN model, but at a given point of space 4 waves only emerge, depending on the local volume fractions. The non-linear pressure waves propagate only in the phase with dominant volume fraction. The new model is tested numerically on various test problems ranging from separated phases in a shock tube to shock – particle cloud interaction. Its predictions are compared to BN and Marble models as well as against experimental data.

**Key words:** hyperbolic, two-phase, compressible, shocks

**Emails:** Richard.Saurel@univ-amu.fr; Ashwin.Chinnayya@ensma.fr; Quentin.Carmouze@rs2n.eu

## I. Introduction

It is well accepted that hyperbolic models are mandatory to deal with phenomena involving wave propagation. This is the case for multiphase flow mixtures in many situations such as in particular shocks and detonations propagation in granular explosives and in fuel suspensions, as well as liquid-gas mixtures with bubbles, cavitation and flashing, as soon as motion is intense and governed by pressure gradients. This is thus the case of most unsteady two-phase flows situations.

Wave propagation is important as it carries pressure, density and velocity disturbances. Sound propagation is also very important as it determines critical (choked) flow conditions and associated mass flow rates. It has also fundamental importance on sonic conditions of detonation waves when the two-phase mixture is exothermically reacting (Petitpas et al., 2009).

Hyperbolicity is also related to the causality principle, meaning that initial and boundary conditions are responsible of time evolution of the solution. When dealing with first-order partial differential equations it means that the Riemann problem must have a solution, and the Riemann problem is correctly posed only if the equations are hyperbolic.

However, only a few two-phase flow models are hyperbolic in the whole range of parameters. The Baer and Nunziato (1986) model seems to be the only formulation able to deal with such requirement. Its symmetric extension (Saurel et al., 2014) facilitates the Riemann problem resolution as the corresponding model involves 7 wave's speeds (instead of 6 in the original version). See also Ambroso et al. (2012) for similar conclusions.

However, in the dilute limit at least, the acoustic properties of this model seem inconsistent (Lhuillier et al., 2013). Indeed with this model, the dispersed phase sound speed corresponds to the one of the pure phase, while this phase is not continuous and unable to propagate sound in reality, at least at a scale larger than particle's one. When the phase is not continuous (dispersed drops in a gas, dispersed bubbles in a liquid), the associated sound speed should vanish, such effect being absent in the formulation.

In the low particles concentration limit, the Marble (1963) model is preferred. This model corresponds to the Euler equations with source terms for the gas phase and pressureless gas dynamic equations for the particle phase (see also Zeldovich, 1970). This model is thermodynamically consistent and hyperbolic as well, except that the particle phase equations are hyperbolic degenerate. In this model, contrarily to the BN model, sound doesn't propagate in the particles phase, this behaviour being more physical in this limit. However, the Marble model has a limited range of validity as the volume of the dispersed phase is neglected, this assumption having sense only for low (less than per cent) condensed phase volume fraction.

There are thus fundamental differences between these two models:

- The volume occupied by the condensed phase is considered in BN while it is neglected in the dilute model, restricting its validity to low dispersed phase volume fractions.
- Condensed phase compressibility is considered in BN while incompressible particles are assumed in the dilute formulation.
- Acoustic properties of the BN model are well accepted in the dense domain but seem inappropriate in the dilute limit.

Even if these two models can be used in the entire space of two-phase flow variables without yielding computational failure (this is characteristic of thermodynamically consistent hyperbolic models) validity of their results is questionable when they are used out of their range of physical validity. This issue has been clearly understood in Lhuillier et al. (2013), McGrath et al. (2016) and Houim and Oran (2016) where various attempts to build new formulations are reported. In Lhuillier et al. (2013) discussion on the volume fraction equation is done, but no explicit flow model is given. In McGrath et al. (2016) a model is given with conditional hyperbolicity. Same issue is present with different cause in Houim and Oran (2016).

The aim of the present paper is to build an alternative to the BN model with improved acoustic properties, while remaining unconditionally hyperbolic and thermodynamically consistent.

The new model is derived from number density and particle radius (or bubble radius) evolution equations resulting in a volume fraction evolution equation expressed in conservation form with

pressure relaxation. Replacing the transport equation in the conventional balance equations of mass, momentum and energy of the phases has dramatic influence on wave's propagation and structure of the equations.

The paper is organised as follows. The well-known BN and Marble models are recalled in Section II to present the main alternatives of existing two-phase hyperbolic models. Derivation of the volume fraction equation of the new model is addressed in Section III. The new model is then derived in Section IV and its hyperbolicity demonstrated. Its compatibility with the model of Kapila et al. (2001) is demonstrated as asymptotic limit of the new model, in the limit of stiff mechanical relaxation. Computed results are then examined in Section V, compared to exact and experimental solutions when available. A symmetric variant of the new flow model, aimed to model bubbly liquids, is derived in Section VI and typical solutions are examined. A general model, aimed to address the full spectrum of volume fractions is then derived in Section VII. Conclusions are given in Section VIII.

## II. Well-known limit models of two-phase flows

Two hyperbolic models are widely used in the two-phase flow literature and their main characteristics are recalled hereafter.

### a) BN type model (1986)

The Baer and Nunziato (1986) model is recalled hereafter, in the absence of granular effects ('configuration' pressure and energy) as well as heat and mass transfers. Mechanical relaxation effects only are considered in addition to waves' dynamics. A variant of this model is available as well in Romenski and Toro (2004), where a conservative formulation is obtained.

The symmetric variant of Saurel et al. (2003) is presented hereafter rather than the original BN.

The evolution equations for phase 1 read,

$$\begin{aligned}
&\frac{\partial \alpha_1}{\partial t} + u_I \frac{\partial \alpha_1}{\partial x} = \mu(p_1 - p_2) \\
&\frac{\partial (\alpha\rho)_1}{\partial t} + \frac{\partial (\alpha\rho u)_1}{\partial x} = 0 \\
&\frac{\partial (\alpha\rho u)_1}{\partial t} + \frac{\partial (\alpha\rho u^2 + \alpha p)_1}{\partial x} = p_I \frac{\partial \alpha_1}{\partial x} + \lambda(u_2 - u_1) \\
&\frac{\partial (\alpha\rho E)_1}{\partial t} + \frac{\partial (\alpha(\rho E + p)u)_1}{\partial x} = p_I u_I \frac{\partial \alpha_1}{\partial x} + \lambda u_I'(u_2 - u_1) - \mu p_I'(p_1 - p_2)
\end{aligned} \qquad \text{(II.1)}$$

The evolution equations of the second phase are,

$$\begin{aligned}
&\frac{\partial (\alpha\rho)_2}{\partial t} + \frac{\partial (\alpha\rho u)_2}{\partial x} = 0 \\
&\frac{\partial (\alpha\rho u)_2}{\partial t} + \frac{\partial (\alpha\rho u^2 + \alpha p)_2}{\partial x} = p_I \frac{\partial \alpha_2}{\partial x} - \lambda(u_2 - u_1) \\
&\frac{\partial (\alpha\rho E)_2}{\partial t} + \frac{\partial (\alpha(\rho E + p)u)_2}{\partial x} = p_I u_I \frac{\partial \alpha_2}{\partial x} - \lambda u_I'(u_2 - u_1) + \mu p_I'(p_1 - p_2)
\end{aligned} \qquad \text{(II.2)}$$

With the following definitions and notations:

- $\alpha_k$, $\rho_k$, $u_k$, $E_k$, $p_k$ denote respectively the volume fraction, material density, velocity, total energy and pressure of the phase k (k=1,2).

- The total energy of the phases reads, $E_k = e_k + \frac{1}{2}u_k^2$.

- The pressures are given by convex equations of state of the form $p_k = p_k(\rho_k, e_k)$.

- The velocities relax each other to a common equilibrium one at a rate controlled by $\lambda$, modelled by conventional drag force correlations and specific interfacial area.

- The pressure relax each other to a common equilibrium one at a rate controlled by $\mu$. Estimates for this relaxation parameter are given in the references above: $\mu = \dfrac{A_I}{Z_1 + Z_2}$, where $A_I$ represents the interfacial exchange area. The specific interfacial area is given by $A_I = \dfrac{3\alpha_1}{R_1}$ if phase 1 represents the dispersed phase made of particles or bubbles of constant radius $R_1$. Obviously, more sophisticated models of interfacial area are possible.
- The interfacial variables are estimated by,

$$u_I = u_I' + \mathrm{sgn}\left(\frac{\partial \alpha_1}{\partial x}\right) \frac{p_2 - p_1}{Z_1 + Z_2} \text{ with } u_I' = \frac{Z_1 u_1 + Z_2 u_2}{Z_1 + Z_2},$$

$$p_I = \frac{Z_2 p_1 + Z_1 p_2}{Z_1 + Z_2} + \mathrm{sgn}\left(\frac{\partial \alpha_1}{\partial x}\right) \frac{Z_1 Z_2}{Z_1 + Z_2}(u_2 - u_1) \text{ with } p_I' = \frac{Z_2 p_1 + Z_1 p_2}{Z_1 + Z_2},$$

where $Z_k = \rho_k c_k$ represents the acoustic impedance of phase k.

This symmetric formulation of the BN model has some advantages:

-Its extension to more than two phases is quite easy.

-It is able to deal with contact and permeable interfaces (Saurel et al., 2003, Saurel et al., 2014).

-It involves an extra wave, not aligned with the condensed phase velocity, this property having benefits at least for numerical resolution (Ambroso et al., 2012, Furfaro and Saurel, 2015).

This system admits the following mixture entropy equation:

$$\frac{\partial (\alpha\rho)_1 s_1 + (\alpha\rho)_2 s_2}{\partial t} + \frac{\partial (\alpha\rho)_1 u_1 s_1 + (\alpha\rho)_2 u_2 s_2}{\partial x} =$$

$$\frac{1}{T_1}\left\{\frac{Z_1}{(Z_1+Z_2)^2}\left((p_2 - p_1) + \mathrm{sgn}\left(\frac{\partial \alpha_1}{\partial x}\right) Z_2 (u_2 - u_1)\right)^2 \left|\frac{\partial \alpha_1}{\partial x}\right| + \lambda \frac{Z_2}{Z_1 + Z_2}(u_2 - u_1)^2 + \mu \frac{Z_1}{Z_1 + Z_2}(p_2 - p_1)^2\right\}$$

$$+\frac{1}{T_2}\left\{\frac{Z_2}{(Z_1+Z_2)^2}\left((p_2 - p_1) + \mathrm{sgn}\left(\frac{\partial \alpha_1}{\partial x}\right) Z_2 (u_2 - u_1)\right)^2 \left|\frac{\partial \alpha_2}{\partial x}\right| + \lambda \frac{Z_1}{Z_1 + Z_2}(u_2 - u_1)^2 + \mu \frac{Z_2}{Z_1 + Z_2}(p_2 - p_1)^2\right\}$$

Its 7 associated wave speeds are:

$\lambda_I = u_I$, $\lambda_1 = u_1$, $\lambda_2 = u_1 + c_1$, $\lambda_3 = u_1 - c_1$, $\lambda_4 = u_2$, $\lambda_5 = u_2 + c_2$, $\lambda_6 = u_2 - c_2$ .

This model is consequently hyperbolic, thermodynamically consistent and symmetric. However, the wave speeds are independent of the volume fraction, meaning that in the dilute limit, the sound speed in the condensed phase is unchanged, this behaviour being questionable as this phase is no longer continuous.

**b) Dilute two-phase flow model (Marble, 1963)**

As the model that follows is no longer symmetric it is necessary to precise the phases. Phase 1 is considered to be the condensed one and the gas phase is denoted by the subscript 2. The 'apparent density' of the dispersed phase is introduced as, $\overline{\rho}_1 = (\alpha\rho)_1$.

In this approach, $\alpha_1 < 0.01$ and volume fraction effects are neglected in the gas phase equations.

Phase 1 (dispersed)

$$\frac{\partial \overline{\rho}_1}{\partial t} + \frac{\partial \overline{\rho}_1 u_1}{\partial x} = 0$$

$$\frac{\partial \overline{\rho}_1 u_1}{\partial t} + \frac{\partial \overline{\rho}_1 u_1^2}{\partial x} = \lambda(u_2 - u_1) \qquad \text{(II.3)}$$

$$\frac{\partial \overline{\rho}_1 e_1}{\partial t} + \frac{\partial \overline{\rho}_1 e_1 u_1}{\partial x} = 0 \text{ or alternatively } \frac{\partial \overline{\rho}_1 E_1}{\partial t} + \frac{\partial \overline{\rho}_1 E_1 u_1}{\partial x} = \lambda u_1 (u_2 - u_1).$$

Phase 2 (gas)

$$\frac{\partial \rho_2}{\partial t} + \frac{\partial \rho_2 u_2}{\partial x} = 0 \qquad \text{(II.4)}$$

$$\frac{\partial \rho_2 u_2}{\partial t} + \frac{\partial \rho_2 u_2^2 + p_2}{\partial x} = -\lambda(u_2 - u_1)$$

$$\frac{\partial \rho_2 E_2}{\partial t} + \frac{\partial (\rho_2 E_2 + p_2) u_2}{\partial x} = -\lambda u_1 (u_2 - u_1)$$

This system admits the following mixture entropy equation:

$$\frac{\partial \overline{\rho}_1 s_1 + \rho_2 s_2}{\partial t} + \frac{\partial \overline{\rho}_1 s_1 u_1 + \rho_2 s_2 u_2}{\partial x} = \frac{\lambda (u_1 - u_2)^2}{T_2}$$

Its associated wave speeds are:

$\lambda_1 = u_1$ , $\lambda_2 = u_2$, $\lambda_3 = u_2 + c_2$, $\lambda_4 = u_2 - c_2$ .

As $\lambda_1 = u_1$ is fold three times, the equations of phase 1 are hyperbolic and linearly degenerate, while the ones of the gas phase are strictly hyperbolic.

These two models are thus well posed in the sense that they are thermodynamically consistent, frame invariant and hyperbolic. Both models can be solved by Godunov type methods as the Riemann problem has been addressed for both (Saurel et al., 1994, Saurel and Abgrall, 1999, Schwendeman et al., 2006, Deledicque and Papalexandris, 2010, Furfaro and Saurel, 2015). However, well posedness is a necessary condition but not a sufficient one for physical validity. In particular, considering again the BN model, the condensed phase sound speed $c_1$ is well defined as a thermodynamic variable and sound disturbances propagate at the particle or grain level. But sound cannot propagate in the mixture at speed $c_1$ as the continuum approximation is no longer valid for the condensed phase as soon as the mixture becomes dilute enough. See also Lhuillier et al. (2013) and McGrath et al. (2016) for further arguments.

**III. Alternative volume fraction equations**

The volume fraction equation of the BN model is the first equation of System (II.1) and can be derived from averaging method considering the transport of a characteristic function, equal to 1 in a given phase and 0 in the other phase. See for example Abgrall and Saurel (2003), Drew and Passman (2006).

Let us now consider another point of view as done by Lhuillier et al. (2013) and consider liquid drops (or condensed phase particles) suspended in a gas. The radius $R_1$ of a single spherical compressible liquid drop surrounded by a gas evolves, under acoustic approximation ($\Delta u \approx \Delta p / \rho c$) with the following transport equation (Chinnayya et al., 2004),

$$\frac{d_1 R_1}{dt} \approx \frac{p_1 - p_2}{\rho_1 c_1}, \qquad \text{(III.1)}$$

where $\frac{d_1}{dt} = \frac{\partial}{\partial t} + u_1 \frac{\partial}{\partial x}$ denotes the Lagrangian derivative of phase 1.

Estimate of the pressure relaxation time $\tau_1$ is given by the time needed for an acoustic wave to travel the particle radius,

$$\tau_1 \approx \frac{R_1}{c_1}.$$

For a liquid drop of 1 mm radius suspended in air the pressure relaxation time is therefore of the order of 1 microsecond. This is very small in most practical situations compared to the other characteristic times related to drag, heat exchange, most situations of wave propagation and fluid motion.

With this definition (III.1) becomes,

$$\frac{d_1 R_1}{dt} \approx \frac{R_1}{\tau} \frac{p_1 - p_2}{\rho_1 c_1^2}$$

Trivial transformation of the former equation implies,

$$\frac{d_1 V_1}{dt} \approx 4\pi R_1^2 \frac{R_1}{\tau_1} \frac{p_1 - p_2}{\rho_1 c_1^2} \qquad \text{(III.2)}$$

where $V_1 = \frac{4}{3}\pi R_1^3$ denotes the volume of the drop.

In absence of fragmentation and coalescence, the specific number of drops per unit volume obeys the following balance equation:

$$\frac{\partial N_1}{\partial t} + \frac{\partial N_1 u_1}{\partial x} = 0, \qquad \text{(III.3)}$$

where $N_1$ represents the specific number of drops.

Multiplying (III.2) by $N_1$ yields,

$$\frac{\partial \alpha_1}{\partial t} + \frac{\partial \alpha_1 u_1}{\partial x} = \frac{3\alpha_1}{\tau_1} \frac{p_1 - p_2}{\rho_1 c_1^2} \qquad \text{(III.4)}$$

as $\alpha_1 = N_1 V_1$.

The volume fraction equation is now in conservative form with a pressure relaxation term.
It is interesting to consider the symmetric situation of liquid containing spherical bubbles.
In this situation the bubble radius evolves according to,

$$\frac{d_2 R_2}{dt} \approx \frac{p_2 - p_1}{\rho_1 c_1},$$

as the acoustic impedance of the less compressible phase ($\rho_1 c_1$) controls the interface velocity.

The specific number of bubbles per unit volume obeys the balance law,

$$\frac{\partial N_2}{\partial t} + \frac{\partial N_2 u_2}{\partial x} = 0,$$

and the corresponding volume fraction equation now reads,

$$\frac{\partial \alpha_2}{\partial t} + \frac{\partial \alpha_2 u_2}{\partial x} = \frac{3\alpha_2}{\tau_2} \frac{p_2 - p_1}{\rho_1 c_1 c_2} \qquad \text{(III.5)}$$

with $\tau_2 \approx \frac{R_2}{c_2}$.

We now examine the implications of such volume fraction equations (III.4 and III.5) on the flow model. The analysis begins with a model based on (III.4) to start with a concrete example.

**IV. The new model**

For the sake of simplicity in the notations and compatibility with (II.1), Equation (III.4) is expressed as

$$\frac{\partial \alpha_1}{\partial t} + \frac{\partial \alpha_1 u_1}{\partial x} = \mu(p_1 - p_2), \qquad \text{(IV.1)}$$

with $\mu = \frac{3\alpha_1}{\tau_1 \rho_1 c_1^2}$, where the estimate for the pressure relaxation time $\tau_1$ has been inserted.

The same mass, momentum and energy equations of Systems (II.1)-(II.2) are reconsidered as,

$$\frac{\partial (\alpha\rho)_1}{\partial t} + \frac{\partial (\alpha\rho u)_1}{\partial x} = 0$$

$$\frac{\partial (\alpha\rho u)_1}{\partial t} + \frac{\partial (\alpha\rho u^2 + \alpha p)_1}{\partial x} = p_I \frac{\partial \alpha_1}{\partial x} + \lambda(u_2 - u_1)$$

$$\frac{\partial(\alpha\rho E)_1}{\partial t}+\frac{\partial(\alpha(\rho E+p)u)_1}{\partial x}=-p_I\frac{\partial\alpha_1}{\partial t}+\lambda u_I(u_2-u_1)+H(T_2-T_1)$$
$$\frac{\partial(\alpha\rho)_2}{\partial t}+\frac{\partial(\alpha\rho u)_2}{\partial x}=0$$
$$\frac{\partial(\alpha\rho u)_2}{\partial t}+\frac{\partial(\alpha\rho u^2+\alpha p)_2}{\partial x}=p_I\frac{\partial\alpha_2}{\partial x}-\lambda(u_2-u_1) \qquad \text{(IV.2)}$$
$$\frac{\partial(\alpha\rho E)_2}{\partial t}+\frac{\partial(\alpha(\rho E+p)u)_2}{\partial x}=p_I\frac{\partial\alpha_1}{\partial t}-\lambda u_I(u_2-u_1)-H(T_2-T_1)$$

The right hand side of the phase energy equations has been modified with the presence of $p_I\frac{\partial\alpha_1}{\partial t}$, the interstitial pressure work, present in (II.1-2) differently.

System (IV.2) obviously satisfies mixture mass, mixture momentum and mixture energy conservation, for any model of interfacial pressure $p_I$ and interfacial velocity $u_I$. Possible estimates are for example (Saurel et al., 2003):

$$p_I=\frac{Z_2p_1+Z_1p_2}{Z_1+Z_2},$$
$$u_I=\frac{Z_1u_1+Z_2u_2}{Z_1+Z_2}, \qquad \text{(IV.3)}$$

Convective heat exchange ($H(T_2-T_1)$) has been inserted for the sake of generality where H denotes the product of the specific interfacial area and heat exchange coefficient, related to the Nusselt number.

Balance equations (IV.2) are considered not only in the BN formulation, but in any two-phase Eulerian model when the effects of volume fraction are considered. The only point to underline is that the various pressures are distinct at this level.

Two questions arise immediately, regarding the fulfilment of the second law of thermodynamics and the hyperbolicity of (IV.1-2). In this aim, the equations are expressed in a set of appropriate variables.

**a) Physical variables formulation**

System (IV.1-2) is expressed with 'physical variables': volume fraction, density, velocity, internal energy and entropy for each phase:

$$\frac{d_1\alpha_1}{dt}+\alpha_1\frac{\partial u_1}{\partial x}=\mu(p_1-p_2) \qquad \text{(IV.4)}$$
$$\frac{d_1\rho_1}{dt}=-\frac{\mu\rho_1}{\alpha_1}(p_1-p_2)$$
$$\frac{d_1u_1}{dt}+\frac{1}{\rho_1}\frac{\partial p_1}{\partial x}=\frac{(p_I-p_1)}{(\alpha\rho)_1}\frac{\partial\alpha_1}{\partial x}+\frac{\lambda(u_2-u_1)}{(\alpha\rho)_1}$$
$$\frac{d_1e_1}{dt}+\frac{p_1-p_I}{\rho_1}\frac{\partial u_1}{\partial x}=-\frac{\mu}{\alpha_1\rho_1}p_I(p_1-p_2)+\frac{\lambda(u_I-u_1)(u_2-u_1)}{(\alpha\rho)_1}+\frac{H(T_2-T_1)}{(\alpha\rho)_1}$$
$$\frac{d_1s_1}{dt}+\frac{p_1-p_I}{\rho_1T_1}\frac{\partial u_1}{\partial x}=-\frac{\mu}{\alpha_1\rho_1T_1}(p_I-p_1)(p_1-p_2)+\frac{\lambda(u_I-u_1)(u_2-u_1)}{(\alpha\rho)_1T_1}+\frac{H(T_2-T_1)}{(\alpha\rho)_1T_1}$$
$$\frac{d_2\rho_2}{dt}+\frac{\rho_2}{\alpha_2}(u_1-u_2)\frac{\partial\alpha_1}{\partial x}+\frac{\alpha_1}{\alpha_2}\rho_2\frac{\partial u_1}{\partial x}+\rho_2\frac{\partial u_2}{\partial x}=\frac{\rho_2}{\alpha_2}\mu(p_1-p_2)$$
$$\frac{d_2u_2}{dt}+\frac{1}{\rho_2}\frac{\partial p_2}{\partial x}=\frac{p_I-p_2}{(\alpha\rho)_2}\frac{\partial\alpha_2}{\partial x}-\frac{\lambda(u_2-u_1)}{(\alpha\rho)_2}$$

$$\frac{d_2 e_2}{dt}+\frac{p_2}{\rho_2}\frac{\partial u_2}{\partial x}+\frac{\alpha_1 p_I}{\alpha_2\rho_2}\frac{\partial u_1}{\partial x}+\frac{p_I(u_1-u_2)}{\alpha_2\rho_2}\frac{\partial \alpha_1}{\partial x}=\frac{\mu p_I(p_1-p_2)}{\alpha_2\rho_2}-\frac{\lambda(u_I-u_2)(u_2-u_1)}{(\alpha\rho)_2}-\frac{H(T_2-T_1)}{(\alpha\rho)_2}$$

$$\frac{d_2 s_2}{dt}+\frac{\alpha_1(p_I-p_2)}{\alpha_2\rho_2 T_2}\frac{\partial u_1}{\partial x}+\frac{(p_I-p_2)(u_1-u_2)}{\alpha_2\rho_2 T_2}\frac{\partial \alpha_1}{\partial x}=\frac{\mu(p_1-p_2)(p_I-p_2)}{\alpha_2\rho_2 T_2}-\frac{\lambda(u_I-u_2)(u_2-u_1)}{(\alpha\rho)_2 T_2}-\frac{H(T_2-T_1)}{(\alpha\rho)_2 T_2}$$

The second equation of this system is particularly interesting. It means that phase 1 density is independent of velocity divergence. As phase 1 is dispersed, there is no reason that droplet cloud contraction or expansion make the density of that phase vary. In the present formulation, it varies only as a consequence of drop contraction or expansion, due to pressure differential.

**b) Stiff pressure relaxation limit**

Former system dramatically simplifies in the stiff pressure relaxation limit, as shown hereafter. Let us consider first-order expansions for the pressures,

$$p_k=\rho_1 c_1^2\left(p_k^0+\varepsilon p_k^1+...\right) \qquad \text{(IV.5)}$$

Where,

- $\varepsilon$ is of the order of the pressure relaxation time ($\varepsilon\approx\tau_1$), tending to zero in most situations ($\varepsilon\to 0^+$),
- $p_k^0$ and $p_k^1$ are respectively the dimensionless pressures at leading and first order of the Taylor expansion.

Inserting these definitions in (III.4) it becomes,

$$\frac{\partial\alpha_1}{\partial t}+\frac{\partial\alpha_1 u_1}{\partial x}=\frac{3\alpha_1}{\varepsilon}(p_1^0+\varepsilon p_1^1-p_2^0-\varepsilon p_2^1)$$

This equation implies two relations, as $\varepsilon$ is arbitrarily small:

$$p_1^0=p_2^0 \qquad \text{(IV.6)}$$

and,

$$\frac{\partial\alpha_1}{\partial t}+\frac{\partial\alpha_1 u_1}{\partial x}=p_1^1-p_2^1 \qquad \text{(IV.7)}$$

The equilibrium condition (IV.6) is valid at leading order only and is different of the strict pressure equilibrium condition,

$$p_1=p_2, \qquad \text{(IV.8)}$$

widely used in two phase flow literature. Such strict equality results in non-hyperbolic models (see for example Guidaglia et al., 2001).

Equation (IV.7) means that pressure fluctuations are still present in the flow model, each time the relaxation coefficient $\mu$ appears in factor of the pressure differential $(p_1-p_2)$.

Let us for example examine the entropy equation of the first phase that becomes, after inserting (IV.5):

$$\frac{d_1 s_1}{dt}+\frac{c_1^2\left(p_1^0-p_I^0\right)}{T_1}\frac{\partial u_1}{\partial x}+\varepsilon\frac{c_1^2\left(p_1^1-p_I^1\right)}{T_1}\frac{\partial u_1}{\partial x}=$$

$$-\frac{3c_1^2}{\varepsilon T_1}\left(p_1^0-p_I^0+\varepsilon(p_1^1-p_I^1)\right)\left(p_1^0-p_2^0+\varepsilon(p_1^1-p_2^1)\right)+\frac{\lambda(u_I-u_1)(u_2-u_1)}{(\alpha\rho)_1 T_1}+\frac{H(T_2-T_1)}{(\alpha\rho)_1 T_1}$$

With the help of (IV.6) simplifications appear,

$$\frac{d_1 s_1}{dt}+\varepsilon\frac{c_1^2\left(p_1^1-p_I^1\right)}{T_1}\frac{\partial u_1}{\partial x}=-\frac{3c_1^2}{T_1}\varepsilon(p_1^1-p_I^1)^2+\frac{\lambda(u_I-u_1)(u_2-u_1)}{(\alpha\rho)_1 T_1}+\frac{H(T_2-T_1)}{(\alpha\rho)_1 T_1}.$$

Under the assumption of smooth solutions and as $\varepsilon\to 0^+$, it reduces to:

$$\frac{d_1 s_1}{dt} = \frac{\lambda(u_I - u_1)(u_2 - u_1)}{(\alpha\rho)_1 T_1} + \frac{H(T_2 - T_1)}{(\alpha\rho)_1 T_1}$$

Therefore all terms involving pressure differential vanish, except those related to first-order pressure relaxation effects (quadratic pressure differential terms vanish). The resulting limit system reads,

$$\frac{d_1 \alpha_1}{dt} + \alpha_1 \frac{\partial u_1}{\partial x} = \mu(p_1 - p_2) \qquad \text{(IV.9)}$$

$$\frac{d_1 \rho_1}{dt} = -\frac{\mu \rho_1}{\alpha_1}(p_1 - p_2)$$

$$\frac{d_1 u_1}{dt} + \frac{1}{\rho_1}\frac{\partial p_1}{\partial x} = \frac{\lambda(u_2 - u_1)}{(\alpha\rho)_1}$$

$$\frac{d_1 e_1}{dt} = -\frac{\mu}{\alpha_1 \rho_1} p_I (p_1 - p_2) + \frac{\lambda(u_I - u_1)(u_2 - u_1)}{(\alpha\rho)_1} + \frac{H(T_2 - T_1)}{(\alpha\rho)_1}$$

$$\frac{d_1 s_1}{dt} = \frac{\lambda(u_I - u_1)(u_2 - u_1)}{(\alpha\rho)_1 T_1} + \frac{H(T_2 - T_1)}{(\alpha\rho)_1 T_1}$$

$$\frac{d_2 \rho_2}{dt} + \frac{\rho_2}{\alpha_2}(u_1 - u_2)\frac{\partial \alpha_1}{\partial x} + \frac{\alpha_1}{\alpha_2}\rho_2 \frac{\partial u_1}{\partial x} + \rho_2 \frac{\partial u_2}{\partial x} = \frac{\rho_2}{\alpha_2}\mu(p_1 - p_2)$$

$$\frac{d_2 u_2}{dt} + \frac{1}{\rho_2}\frac{\partial p_2}{\partial x} = -\frac{\lambda(u_2 - u_1)}{(\alpha\rho)_2}$$

$$\frac{d_2 e_2}{dt} + \frac{p_2}{\rho_2}\frac{\partial u_2}{\partial x} + \frac{\alpha_1 p_I}{\alpha_2 \rho_2}\frac{\partial u_1}{\partial x} + \frac{p_I(u_1 - u_2)}{\alpha_2 \rho_2}\frac{\partial \alpha_1}{\partial x} = \frac{\mu p_I (p_1 - p_2)}{\alpha_2 \rho_2} - \frac{\lambda(u_I - u_2)(u_2 - u_1)}{(\alpha\rho)_2} - \frac{H(T_2 - T_1)}{(\alpha\rho)_2}$$

$$\frac{d_2 s_2}{dt} = -\frac{\lambda(u_I - u_2)(u_2 - u_1)}{(\alpha\rho)_2 T_2} - \frac{H(T_2 - T_1)}{(\alpha\rho)_2 T_2}$$

With the help of interfacial variables estimates (IV.3) the entropy equations become,

$$\frac{d_1 s_1}{dt} = \frac{\lambda}{(\alpha\rho)_1 T_1}\frac{Z_2}{Z_1 + Z_2}(u_2 - u_1)^2 + \frac{H(T_2 - T_1)}{(\alpha\rho)_1 T_1}$$

$$\frac{d_2 s_2}{dt} = \frac{\lambda}{(\alpha\rho)_2 T_2}\frac{Z_1}{Z_1 + Z_2}(u_2 - u_1)^2 - \frac{H(T_2 - T_1)}{(\alpha\rho)_2 T_2}$$

Combination of these equations with the mass equations results in the following mixture entropy equation, that guarantees non-negative evolutions,

$$\frac{\partial \alpha_1\rho_1 s_1 + \alpha_2\rho_2 s_2}{\partial t} + \frac{\partial \alpha_1\rho_1 s_1 u_1 + \alpha_2\rho_2 s_2 u_2}{\partial x} = \left(\frac{Z_2}{T_1} + \frac{Z_1}{T_2}\right)\frac{\lambda}{Z_1 + Z_2}(u_2 - u_1)^2 + \frac{H(T_2 - T_1)^2}{T_1 T_2} \qquad \text{(IV.10)}$$

System (IV.9) is consequently entropy preserving.

It is interesting to note that, in the present limit, the internal energy equation of the first phase expresses in conservation form:

$$\frac{\partial \alpha_1\rho_1 e_1}{\partial t} + \frac{\partial \alpha_1\rho_1 e_1 u_1}{\partial x} = -\mu p_I (p_1 - p_2) + \lambda(u_I - u_1)(u_2 - u_1) + H(T_2 - T_1) \qquad \text{(IV.11)}$$

We now check hyperbolicity of the same equations.

### c) Hyperbolicity

System (IV.9) in absence of relaxation effects, is expressed as,

$$\frac{\partial W}{\partial t} + A(W)\frac{\partial W}{\partial x} = 0,$$

with,

$$W = (\rho_1,\ s_1,\ s_2,\ \alpha_1,\ u_1,\ \rho_2,\ u_2)^T.$$

The Jacobian matrix reads,

$$A(W) = \begin{pmatrix} u_1 & 0 & 0 & 0 & 0 & 0 & 0 \\ 0 & u_1 & 0 & 0 & 0 & 0 & 0 \\ 0 & 0 & u_2 & 0 & 0 & 0 & 0 \\ 0 & 0 & 0 & u_1 & \alpha_1 & 0 & 0 \\ \dfrac{c_1^2}{\rho_1} & \dfrac{1}{\rho_1}\dfrac{\partial p_1}{\partial s_1}\Big)_{\rho_1} & 0 & 0 & u_1 & 0 & 0 \\ 0 & 0 & 0 & \dfrac{\rho_2}{\alpha_2}(u_1 - u_2) & \dfrac{\alpha_1}{\alpha_2}\rho_2 & u_2 & \rho_2 \\ 0 & 0 & \dfrac{1}{\rho_2}\dfrac{\partial p_2}{\partial s_2}\Big)_{\rho_2} & 0 & 0 & \dfrac{c_2^2}{\rho_2} & u_2 \end{pmatrix}.$$

The wave speeds, solution of $|A - \lambda I| = 0$ are,

$$\lambda_{1-4} = u_1,\ \lambda_5 = u_2,\ \lambda_6 = u_2 - c_2 \text{ and } \lambda_7 = u_2 + c_2\ . \qquad \text{(IV.12)}$$

All roots being real the system is unconditionally hyperbolic. The wave speeds correspond to the one of the dilute model of Marble (1963) (Systems II.2 – II.3) and not those of Baer and Nunziato (1986), as expected.

**d) Model summary**

The flow model thus consists in System (IV.1-2) with the condition:

$$\tau_1 \to 0^+ \qquad \text{(IV.13)}$$

Alternatively it can be expressed as,

$$\begin{aligned}
&\frac{\partial \alpha_1}{\partial t} + \frac{\partial \alpha_1 u_1}{\partial x} = \mu(p_1 - p_2), \qquad \text{with } \mu \to +\infty \\
&\frac{\partial (\alpha\rho)_1}{\partial t} + \frac{\partial (\alpha\rho u)_1}{\partial x} = 0, \\
&\frac{\partial \alpha_1\rho_1 u_1}{\partial t} + \frac{\partial \alpha_1\rho_1 u_1^2 + \alpha_1 p_1}{\partial x} = p_I \frac{\partial \alpha_1}{\partial x} + \lambda(u_2 - u_1), \\
&\frac{\partial \alpha_1\rho_1 e_1}{\partial t} + \frac{\partial \alpha_1\rho_1 u_1 e_1}{\partial x} = -\mu p_I (p_1 - p_2) + \lambda \frac{Z_2}{Z_1 + Z_2}(u_2 - u_1)^2 + H(T_2 - T_1), \\
&\frac{\partial (\alpha\rho)_2}{\partial t} + \frac{\partial (\alpha\rho u)_2}{\partial x} = 0, \qquad \text{(IV.14)} \\
&\frac{\partial (\alpha_1\rho_1 u_1 + \alpha_2\rho_2 u_2)}{\partial t} + \frac{\partial (\alpha_1\rho_1 u_1^2 + \alpha_1 p_1) + (\alpha_2\rho_2 u_2^2 + \alpha_2 p_2)}{\partial x} = 0, \\
&\frac{\partial (\alpha_1\rho_1 E_1 + \alpha_2\rho_2 E_2)}{\partial t} + \frac{\partial \alpha_1 u_1(\rho_1 E_1 + p_1) + \alpha_2 u_2(\rho_2 E_2 + p_2)}{\partial x} = 0.
\end{aligned}$$

In this formulation there is a single non-conservative equation (the momentum one of the liquid phase) as the momentum of the second phase is deduced from the mixture momentum equation. The conservative internal energy equation for the liquid phase is a consequence of the second equation of (IV.4) and stiff pressure relaxation limit. This is a nice property that may simplify shock conditions determination. Obviously, System (IV.14) can be complemented by mass transfer.

**e) Stiff mechanical relaxation limit**

We now address both stiff pressure and velocity relaxation limit to check compatibility of the model with the Kapila et al. (2001) one. This is important for the computation of material interfaces with capturing methods. Here, only pressure and velocity relaxation processes are considered. They are considered to relax at infinite rate.

The pressure evolution equations read,

$$\frac{\partial p_1}{\partial t} + u_1 \frac{\partial p_1}{\partial x} = -\frac{\rho_1 c_1^2}{\alpha_1} \mu (p_1 - p_2)$$

$$\frac{\partial p_2}{\partial t} + u_2 \frac{\partial p_2}{\partial x} + \frac{\rho_2 c_2^2}{\alpha_2} \frac{\partial \alpha_1 u_1 + \alpha_2 u_2}{\partial x} = \frac{\rho_2 c_2^2}{\alpha_2} \mu (p_1 - p_2)$$

Taking the difference,

$$u_1 \frac{\partial p_1}{\partial x} - u_2 \frac{\partial p_2}{\partial x} - \frac{\rho_2 c_2^2}{\alpha_2} \frac{\partial \alpha_1 u_1 + \alpha_2 u_2}{\partial x} = -\left( \frac{\rho_1 c_1^2}{\alpha_1} + \frac{\rho_2 c_2^2}{\alpha_2} \right) \mu (p_1 - p_2) .$$

In the stiff pressure ($p_1^0 = p_2^0 = p^0$) and velocity relaxation limits ($u_1^0 = u_2^0 = u^0$),

$$\mu (p_1 - p_2) \to \frac{\dfrac{\rho_2 c_2^2}{\alpha_2}}{\dfrac{\rho_1 c_1^2}{\alpha_1} + \dfrac{\rho_2 c_2^2}{\alpha_2}} \frac{\partial u}{\partial x}$$

Inserting this result in the volume fraction equation,

$$\frac{\partial \alpha_1}{\partial t} + u \frac{\partial \alpha_1}{\partial x} = \frac{\dfrac{\rho_1 c_1^2 - \rho_2 c_2^2}{\alpha_2}}{\dfrac{\rho_1 c_1^2}{\alpha_1} + \dfrac{\rho_2 c_2^2}{\alpha_2}} \frac{\partial u}{\partial x} ,$$

the volume fraction equation of the Kapila et al. (2001) model is recovered.

The mixture sound speed at mechanical equilibrium is thus that of Wood (1930), $\dfrac{1}{\rho c^2} = \dfrac{\alpha_1}{\rho_1 c_1^2} + \dfrac{\alpha_2}{\rho_2 c_2^2}$ while for the Marble model with stiff velocity relaxation, the mechanical equilibrium sound speed is $c^2 = \left( \dfrac{\rho_2}{\rho} \right) c_2^2$, which is very different.

As the Kapila model is recovered in the stiff mechanical relaxation limit, it means that the present flow model is able to compute interfacial flows with the help of stiff velocity and pressure relaxation solvers. This feature is particularly important for the sake of generality of the formulation.

The present model is hyperbolic but not symmetric, as sound propagates only with the second phase. It is therefore interesting to compute relevant test problems to examine typical solutions. To do this, an appropriate flow solver is derived in Appendix A.

## V. Computed results

Several test problems are addressed, some giving relevant illustrations of model's capabilities, other serving for validation as compared to exact solutions as well as experimental data.

### Shock tube tests

The first test corresponds to the simple transport of a volume fraction discontinuity in a flow field in uniform pressure and velocity equilibrium. The method of Appendix A is extended to higher order thanks to the MUSCL algorithm (see for example Toro, 1997). Present computations use the Minmod

limiter. The ideal gas equation of state is used to model thermodynamics of the gas phase, while the liquid is modeled by the stiffened gas EOS. These two EOS can be summarized as follows,

$$p_k(\rho_k, e_k) = (\gamma_k - 1)\rho_k e_k - \gamma_k p_{\infty k}, \qquad \text{(V.1)}$$

with following sets or parameters,

$\gamma_{air} = 1.4$, $p_{\infty,air} = 0$, k=air,

$\gamma_{water} = 4.4$, $p_{\infty,water} = 6\,10^8\,Pa$, k=liquid water.

These equations of state and associated parameters are used in all test problems of the present section.
A volume fraction discontinuity separating two mixtures is transported at 100 m/s in a uniform pressure flow field of 0.1 MPa. The initial discontinuity is located at 0.5 m initially and computed results are compared to the exact solution at time 1 ms in the Figure 1.

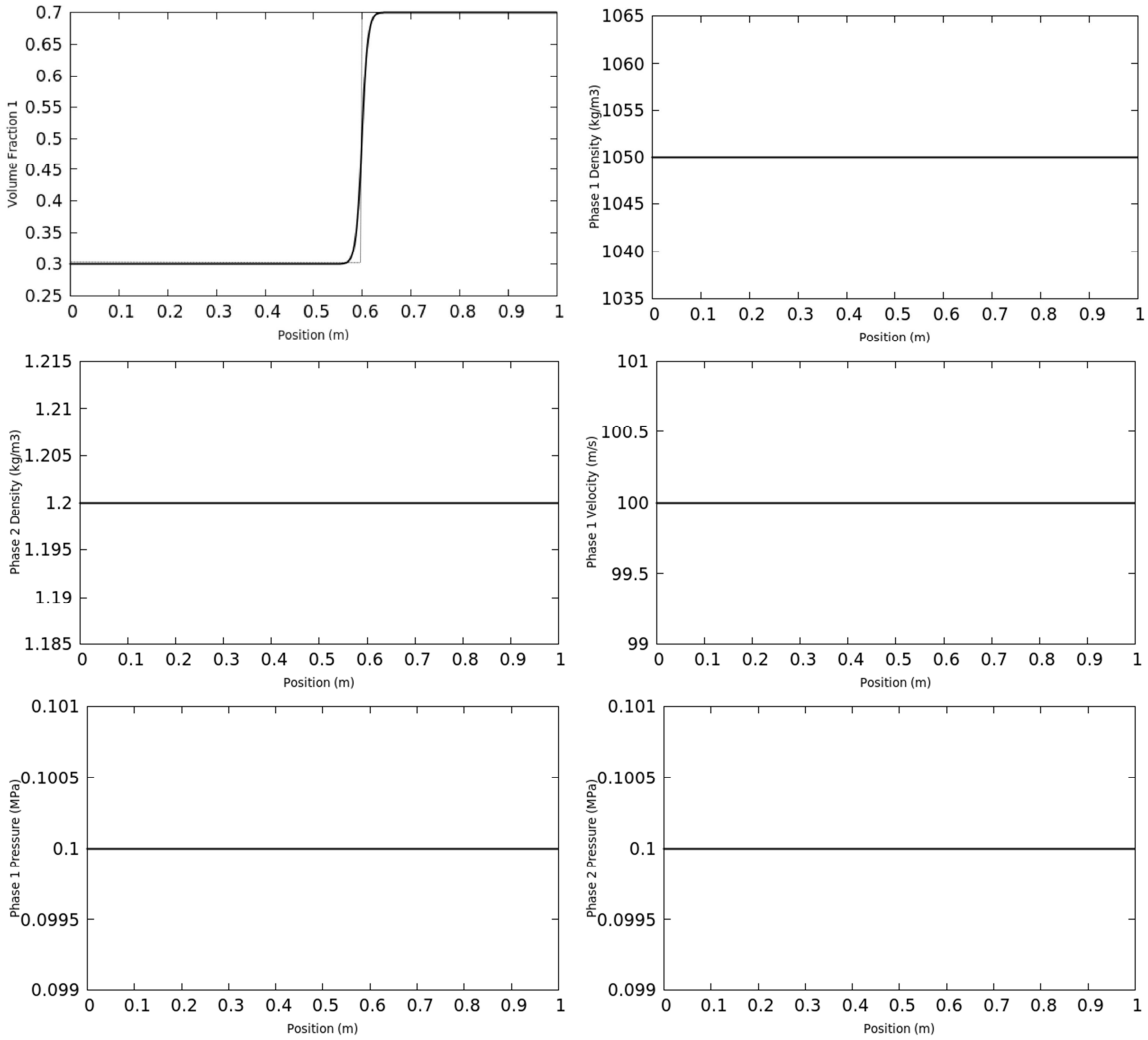


**Figure 1.** Volume fraction transport in uniform pressure and velocity fields. The mesh involves 500 cells and the time step is computed with CFL=0.5. Initial velocities are set to 100m/s and pressures are constant and equal to $10^5$ Pa. The volume fraction discontinuity is initially set at 0.5 m. The numerical solution is plotted at 1ms. The exact solution for the volume fraction is presented in dot symbols showing perfect agreement. The numerical solutions are oscillations free.

Another test is now addressed and corresponds to a two phase shock tube, as shown in Figure 2. In this test, stiff pressure relaxation is not used, while the flow model is hyperbolic and entropy preserving only when stiff pressure relaxation is done. Consequently, the present computations should fail. They however produce results with quite significant pressure disequilibrium, showing robustness of the formulation.

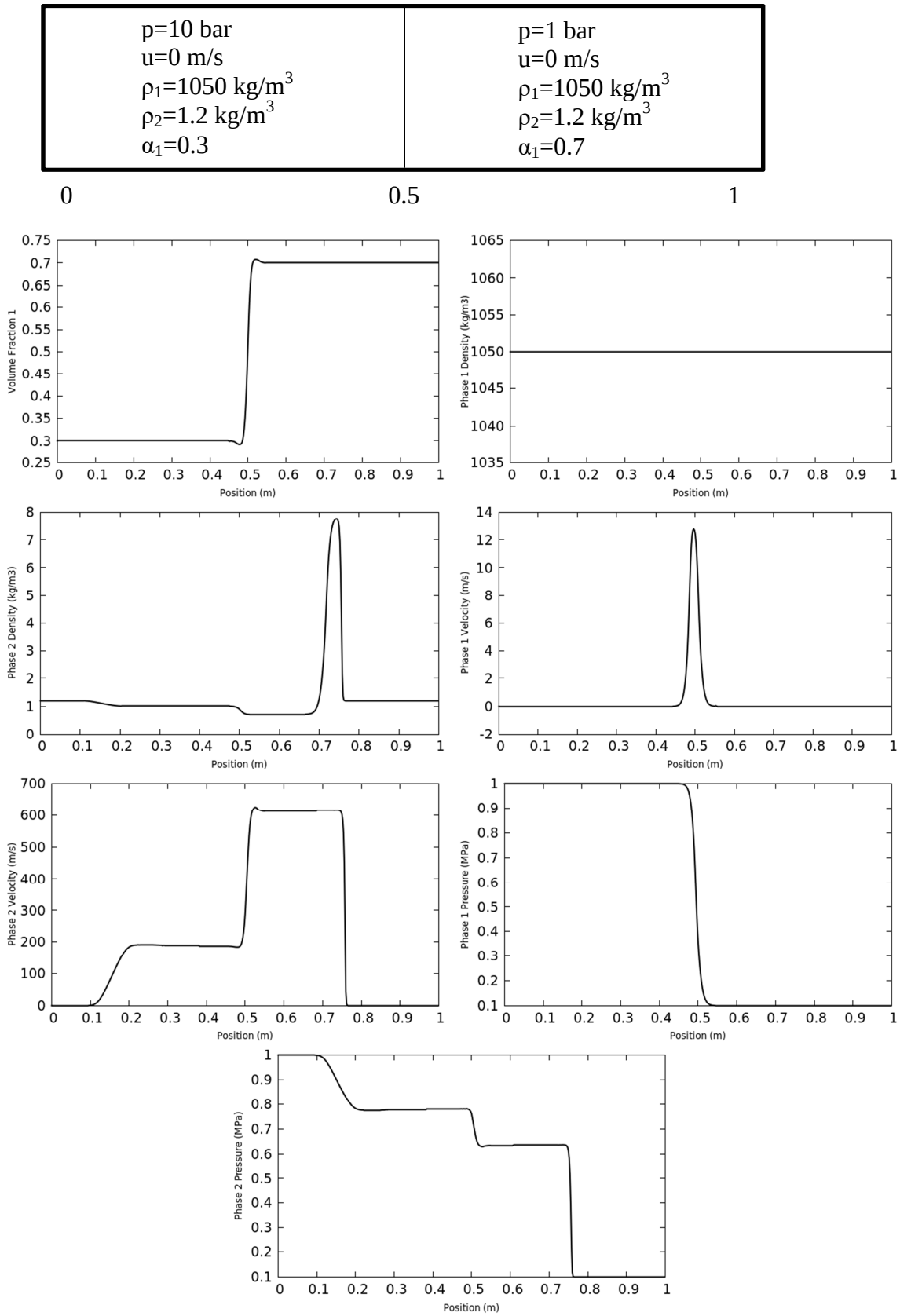


**Figure 2**. "Smooth shock tube test case". Computations are made in the absence of relaxation terms, with 500 cells and CFL=0.5. Results are shown at time 350μs. Four waves are visible, in spite of the simplified Riemann solver that considers two only. It is interesting to note the discontinuous profile of pressure in the phase 1: no pressure wave is present in this phase. Phase 1 shows slight velocity creation

(compared to the velocity of the gas phase) even in absence of drag, the pressure term in the momentum equation being responsible for that.

These typical profiles are very different to those expected with BN and Marble models (without relaxation terms). For example, the pressure profiles of the phases are very different and even unphysical, but the model and algorithm do not fail.
To recover acceptable pressure evolutions in the condensed phase, stiff pressure relaxation is used. Pressure and velocity relaxation solvers are recalled in Appendix B.
The same run as the one defined in Figure 2 is reconsidered hereafter with pressure relaxation and the results are shown in Figure 3.

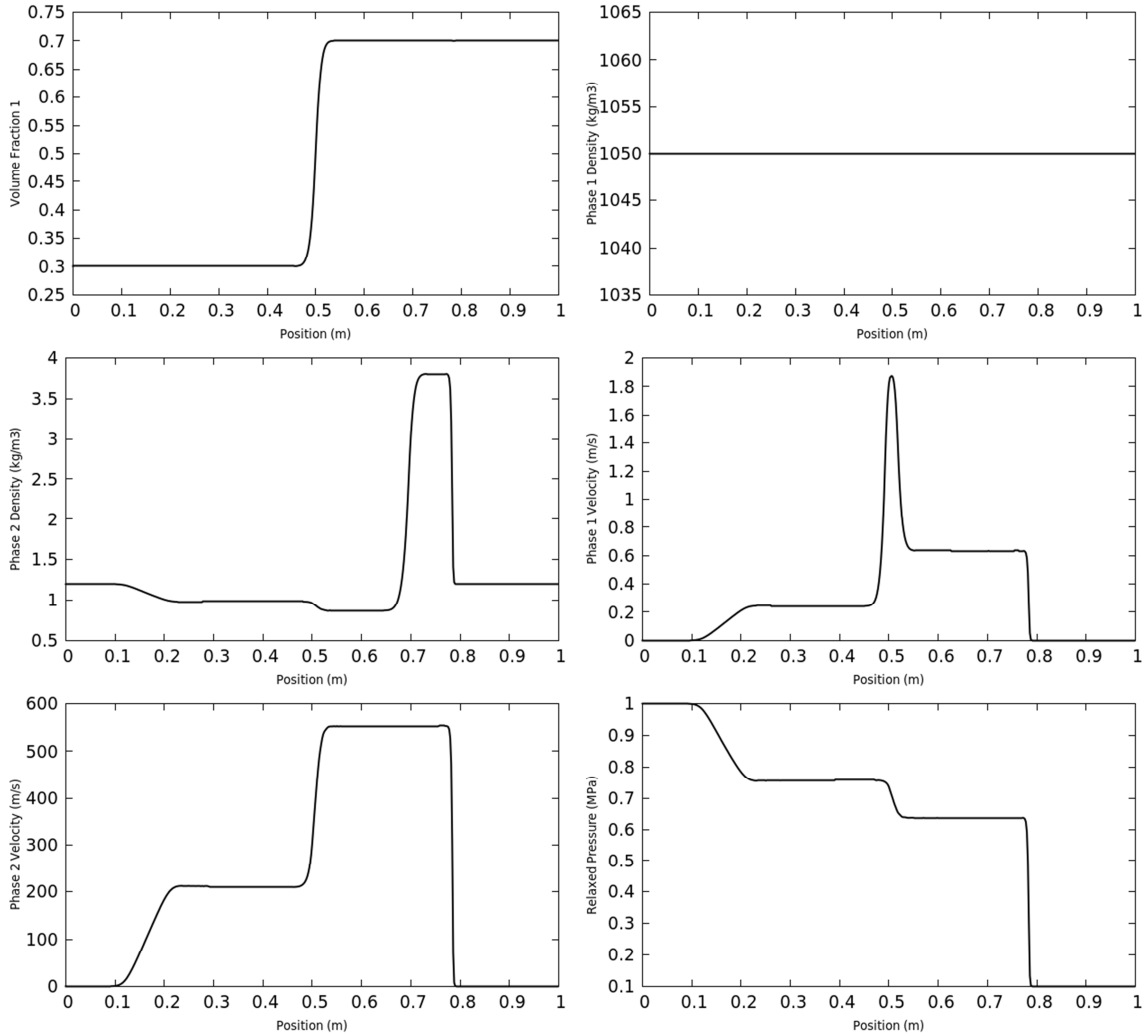


**Figure 3.** Smooth shock tube computations in the absence of velocity relaxation but with stiff pressure relaxation. Computations made with 500 cells and CFL=0.5. Computed results are shown at time 350µs. All pressures are now equal, modifying significantly the phase 1 velocity profile.

With the help of both velocity and pressure relaxation solvers it is possible to address interfaces separating (nearly) pure liquid and (nearly) pure gas. The aim is to analyze the behavior of the flow model in another limit case, having in mind it has been derived for clouds of droplets, not interfaces. The initial conditions are given in Figure 4 and correspond to a liquid at right set to motion by a pressurized gas at left. The exact solution is available for this test case and used to check accuracy of computations.

| | |
|---|---|
| p=10 000 bar<br>u=0 m/s<br>$\rho_1$=1050 kg/m$^3$<br>$\rho_2$=100 kg/m$^3$<br>$\alpha_1$=0.0001 | p=1 bar<br>u=0 m/s<br>$\rho_1$=1050 kg/m$^3$<br>$\rho_2$=100 kg/m$^3$<br>$\alpha_1$=0.9999 |

0 0.6 1

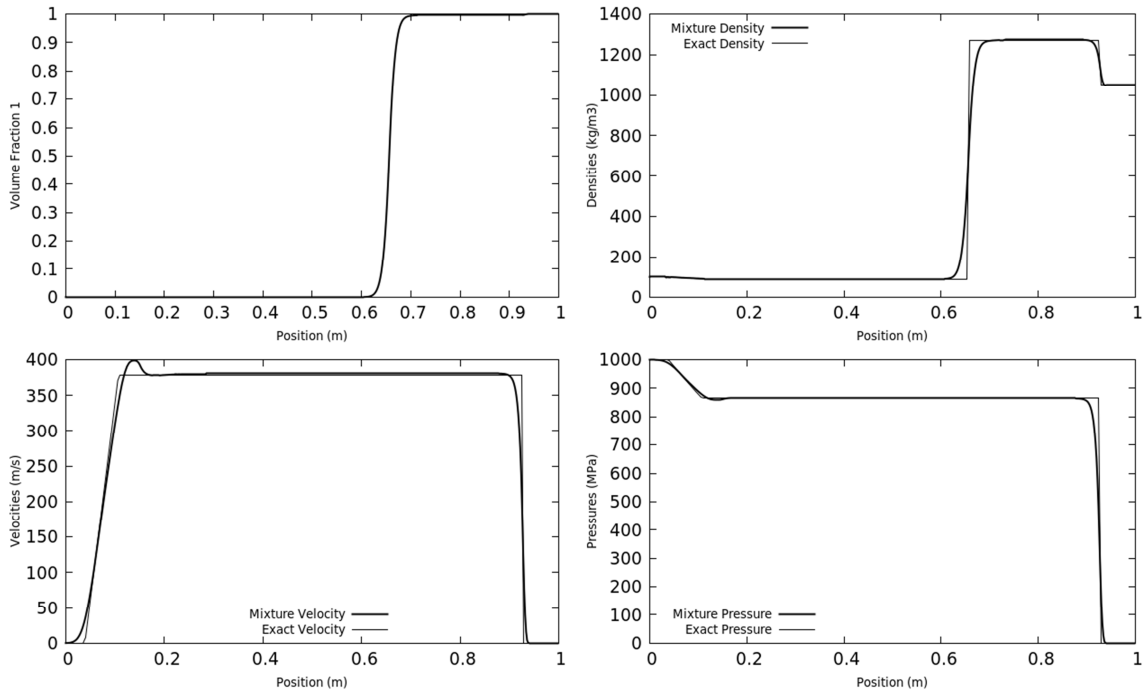


**Figure 4.** Shock tube with gas-liquid interface: High pressure gas at left and low pressure liquid at right. Computations done with 500 cells and CFL=0.5. Computed results shown at time 150μs. Both velocities and pressure are relaxed, making the interface condition of equal pressures and velocities fulfilled.

The same test is considered but with fluids in reverse order: High pressure liquid at left and low pressure gas at right. This test is more severe as maintaining pressure positivity during liquid expansion is hard to manage. Corresponding results are shown in Figure 5 and compared to the exact solution.

| | |
|---|---|
| p=10 000 bar<br>u=0 m/s<br>$\rho_1$=1050 kg/m$^3$<br>$\rho_2$=100 kg/m$^3$<br>$\alpha_1$=0.9999 | p=1 bar<br>u=0 m/s<br>$\rho_1$=1050 kg/m$^3$<br>$\rho_2$=100 kg/m$^3$<br>$\alpha_1$=0.0001 |

0 0.7 1

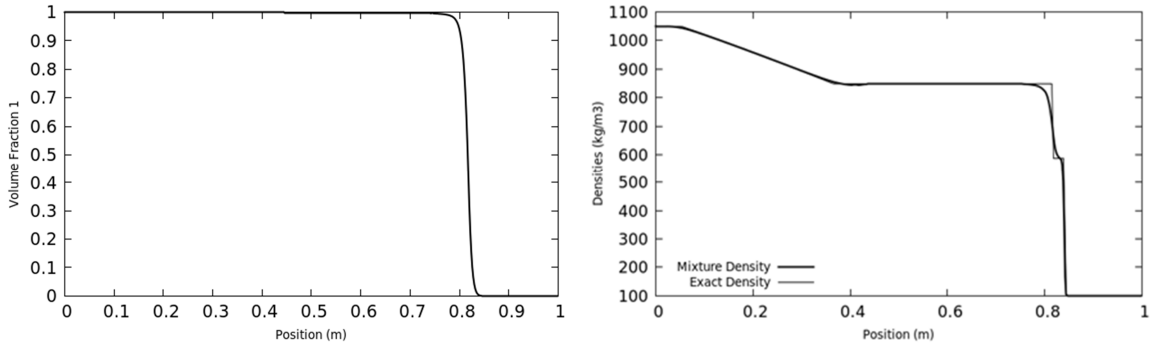

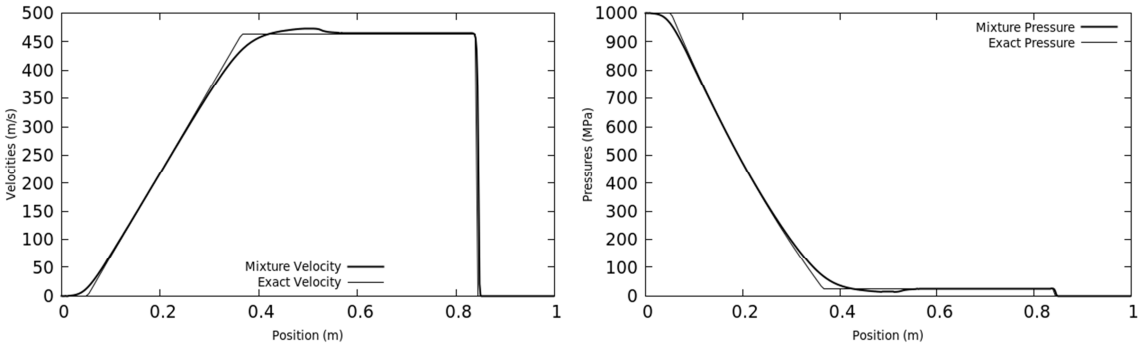


**Figure 5.** Shock tube with liquid-gas interface: high pressure liquid at left and low pressure gas at right. Computations done with 500 cells and CFL=0.5. Computed results shown at time 250μs. Both velocities and pressure are relaxed, making the interface condition of equal pressures and velocities fulfilled.

These various results illustrate method's capabilities in several configurations far from the original design of the model, based on clouds of droplets suspended in air. It is also interesting to note that even if the liquid acoustic wave is absent of the formulation, its dynamics is correctly computed thanks to relaxation effects.

**Shock interaction with a fluidized bed – Rogue test**

We now consider a test more appropriate to the model. It consists in the fluidization of a particle cloud under shock wave interaction. Such a configuration has been studied experimentally by Rogue et al. (1998) and is summarized in Figure 6.

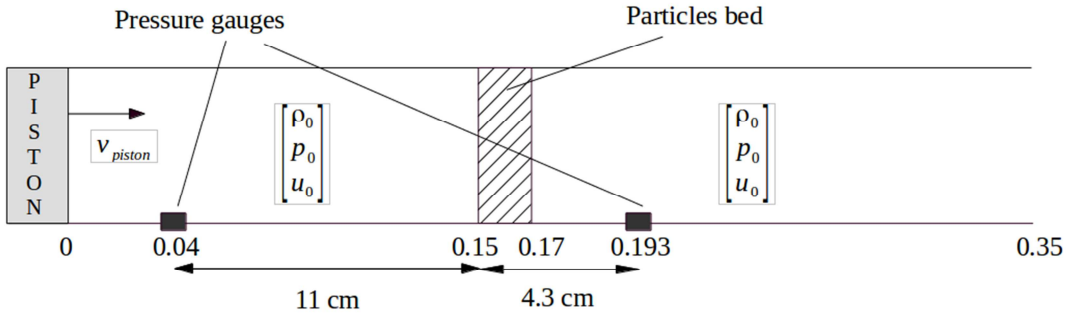


**Figure 6.** Rogue et al. (1998) fluidization shock tube test. A shock tube is filled with gas at density 1.2 kg/m$^3$. A dense cloud of nylon particles ($\rho_0 = 1050 \text{kg/m}^3$) is set in a cross section of the tube, with 2 cm width. The initial solid volume fraction in the particle bed is 0.65. The initial pressure is uniform initially and set at $10^5$ Pa. A shock at Mach number 1.3 is created by the expansion of the high pressure gas, equivalent to a shock created by a piston moving at 151 m/s.

In this experiment pressure signals are recorded before and after the particles cloud, to examine reflected and transmitted waves through the granular media as well as its dilution and dispersion.

To account for drag effects the following correlation is used, combination of Ergun (1952) and Bernecker and Price (1974),

$$F = \frac{\rho_2}{d_1} C_d \left| u_2 - u_1 \right| \left( u_2 - u_1 \right)$$

with,

$$C_d = \begin{cases} \dfrac{150\alpha_1}{Re} + 1.75 & \text{if} \quad \alpha_1 \geq \alpha_{cr} \\ \dfrac{150\alpha_1}{Re} + 1.75\left[\dfrac{(1-\alpha_{cr})\alpha_1}{\alpha_1\alpha_2}\right]^{0.45} & \text{if} \quad (1\text{-}\alpha_s) \leq \alpha_1 \leq \alpha_{cr} \\ \dfrac{150\alpha_1}{Re} + 0.3 & \text{if} \quad \alpha_1 \leq (1\text{-}\alpha_s) \end{cases},$$

$R_e = \dfrac{\alpha_2\rho_2|u_2-u_1|d_1}{\mu_2}$ the particulate Reynolds number, $\alpha_{cr} = 0.63$ and $\alpha_s = \left(1+0.02\dfrac{1-\alpha_{cr}}{\alpha_{cr}}\right)^{-1}$.

The particle diameter appearing in these relations is constant ($d_1 = 1.5mm$) and the gas viscosity is $\mu_2 = 1810^{-6}$ Pa.s.

The granular bed is made of nylon particles, treated as compressible material, governed by the SG EOS (V.1) with the same EOS parameters as liquid water.

Predictions of the BN, Marble and new model are compared with the same modeling of drag effects given above. The BN model, or more precisely its symmetric version with 7 waves is solved with the Furfaro and Saurel (2015) method. The Marble model is solved with the Saurel et al. (1994) method and the new model is solved with the method presented above.

Let us first comment Rogue et al. (1998) experimental data, typical pressure signals being shown in Figure 7.

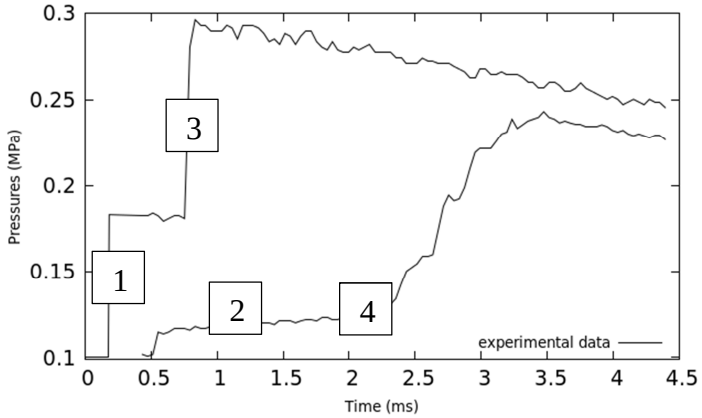


**Figure 7.** Experimental pressures signals of Rogue (1998): 1 denotes the incident shock wave, 2 denotes the transmitted shock wave/fan of compression waves, 3 denotes the reflected shock wave on the particles cloud, 4 corresponds to the arrival of the cloud upper front at the pressure gauge location.

Computed results with the various flow models are shown in Figure 8.

(Marble) (BN)

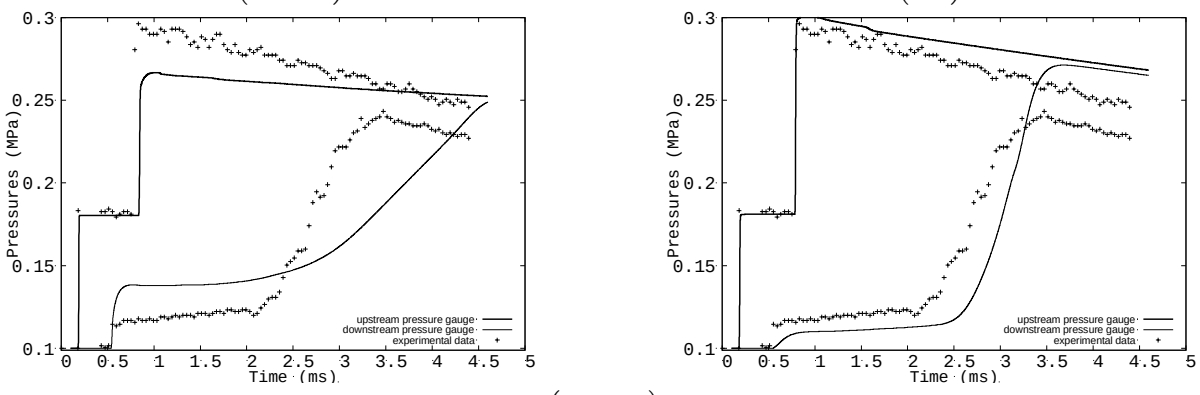


(present)

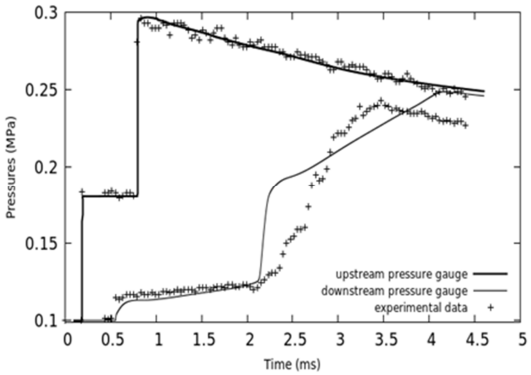


**Figure 8.** Comparison of computed results with the various models (lines) versus experimental data (symbols) for the Rogue test problem. Computations are done with 1000 cells and CFL=0.5. The Minmod flux limiter is used in the MUSCL method. Reflected and transmitted waves are badly predicted with the Marble model. Wave transmission and reflection are better with BN. Wave's dynamics is considerably improved with the with the new model, but cloud's dynamics is still perfectible.

At this stage, more potential than expected appeared with the various shock tube tests in limit configurations, but weakness appeared for particle cloud dynamics in the Rogue test.
A symmetric variant of the new model, with Equation (III.5) instead of (III.4) is thus considered and examined.

## VI. Symmetric variant

In the model examined and tested formerly pressure waves propagate with the gas sound speed. This behavior seems incorrect if the flow is mainly liquid, which is the continuous phase with bubbly flows. We thus address the symmetric variant of the previous model on the basis of the volume fraction equation (III.5).
Equation (III.5) is thus plugged to the system of balance equations (IV.2). Analysis of the resulting system yields the following wave's speeds:
$\lambda_{1-4} = u_2$ , $\lambda_5 = u_1$ , $\lambda_6 = u_1 - c_1$ and $\lambda_7 = u_1 + c_1$ .
We examine typical solutions on some test problems, as done previously.
The same shock tube test case as the one of Figure 5 is considered with liquid at left and gas at right. Computed results are compared against the exact solution in Figure 9 at the same time 250μs.

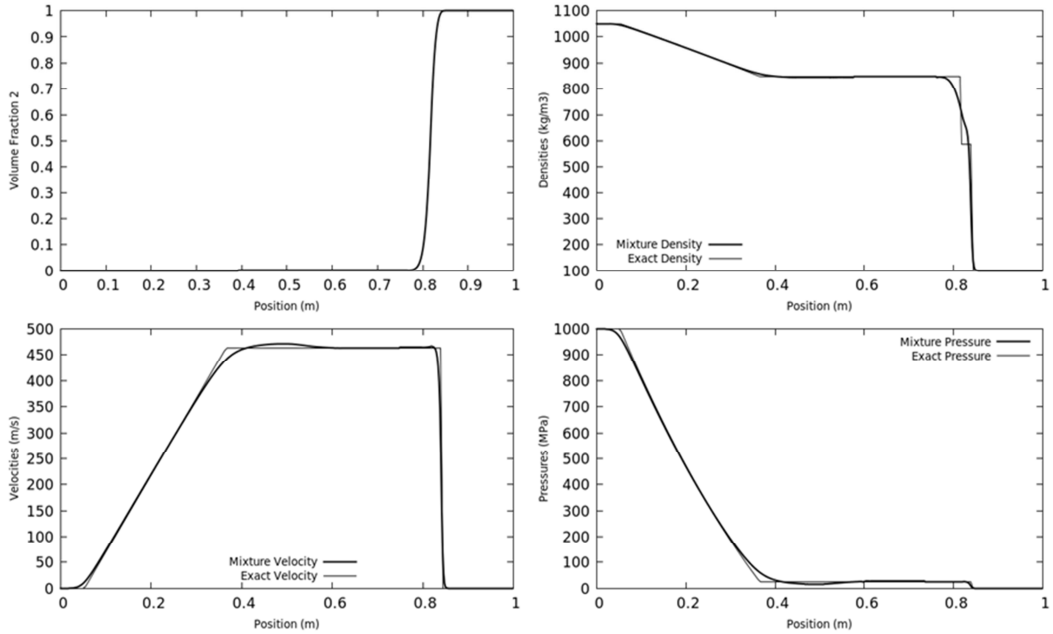

**Figure 9.** Liquid – gas shock tube test problem solved with the symmetric variant model with stiff pressure and velocity relaxation. Computations are done with 500 cells and CFL=0.5. Results are shown at time 250μs. The numerical solution tends to the exact one but converges more difficultly, as visible on the density graph.

This test is however interesting as the wave dynamics in the gas phase is correctly computed, while it is absent of the non-equilibrium flow model.
It is also interesting to address the Rogue test problem with the symmetric variant model. Corresponding results are shown in Figure 10, showing improvement of the pressure evolution in the cloud dynamics, but poor wave propagation in the gas phase. This test shows the limits of the pressure relaxation method, to rebuilt an acoustic wave absent of the original hyperbolic system.

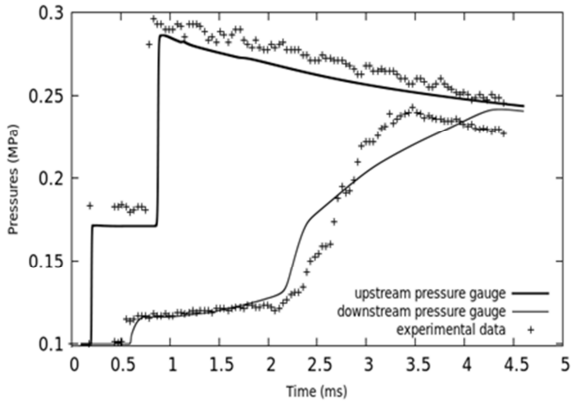


**Figure 10.** Computed pressure profiles of the Rogue test with the symmetric variant model (lines) are compared against pressure records (symbols). Computations are done with 1000 cells and CFL=0.5. Accuracy has been lost in the incident and reflected waves compared to the former model while an interesting feature appears regarding the beginning of the pressure rise during particle cloud motion that seems more accurate.

The lack of accuracy in the incident shock that propagates in a single phase gas media is due to the absence of gas sound speed in the eigenvalues. Also, the present formulation is derived for bubbly flows while it is used for a nearly pure gas in the first part of the shock tube. Therefore an attempt for a general formulation is done in the section that follows.

## VII. Towards a general formulation

The new model and its symmetric variant are embedded in a general formulation. Parameters 'a' and 'b' are defined as,

$$a = \begin{cases} 1 & \text{if} \quad \alpha_1 < \alpha^{\text{fluidization}} \\ 0 & \text{otherwize} \end{cases} \qquad \text{(VII.1)}$$

$$b = a - 1$$

Parameter $\alpha^{\text{fluidization}}$ corresponds to some fluidization limit, for example $\alpha^{\text{fluidization}} \approx 0.5$. This parameter has been used in the various computations that will be examined later. The various tests done haven't shown clear dependence to this parameter.
Therefore, in this formulation 'a' and 'b' are local constants, but as they vary in space as $a = a(\alpha_1)$ and $b = b(\alpha_1)$.
The general flow model reads,

$$\frac{\partial \alpha_1}{\partial t} + a\frac{\partial \alpha_1 u_1}{\partial x} + b\frac{\partial \alpha_2 u_2}{\partial x} = \mu(p_1 - p_2), \qquad \text{(VII.2)}$$

$$\frac{\partial(\alpha\rho)_1}{\partial t} + \frac{\partial(\alpha\rho u)_1}{\partial x} = 0$$

$$\frac{\partial \alpha_1\rho_1 u_1}{\partial t} + \frac{\partial \alpha_1\rho_1 u_1^2 + \alpha_1 p_1}{\partial x} = p_I \frac{\partial \alpha_1}{\partial x} + \lambda(u_2 - u_1)$$

$$\frac{\partial \alpha_1\rho_1 E_1}{\partial t} + \frac{\partial \alpha_1\rho_1 u_1 E_1}{\partial x} + \frac{\partial \alpha_1 u_1 p_1}{\partial x} = p_I\left(a\frac{\partial \alpha_1 u_1}{\partial x} + b\frac{\partial \alpha_2 u_2}{\partial x}\right) - p_I\mu(p_1 - p_2) + \lambda u_I(u_2 - u_1) + H(T_2 - T_1)$$

$$\frac{\partial(\alpha\rho)_2}{\partial t} + \frac{\partial(\alpha\rho u)_2}{\partial x} = 0$$

$$\frac{\partial \alpha_2\rho_2 u_2}{\partial t} + \frac{\partial \alpha_2\rho_2 u_2^2 + \alpha_2 p_2}{\partial x} = p_I \frac{\partial \alpha_2}{\partial x} - \lambda(u_2 - u_1)$$

$$\frac{\partial \alpha_2\rho_2 E_2}{\partial t} + \frac{\partial \alpha_2\rho_2 u_2 E_2}{\partial x} + \frac{\partial \alpha_2 u_2 p_2}{\partial x} = -p_I\left(a\frac{\partial \alpha_1 u_1}{\partial x} + b\frac{\partial \alpha_2 u_2}{\partial x}\right) + p_I\mu(p_1 - p_2) - \lambda u_1(u_2 - u_1) - H(T_2 - T_1)$$

It admits the following additional mixture entropy equation,

$$\frac{\partial \alpha_1\rho_1 s_1 + \alpha_2\rho_2 s_2}{\partial t} + \frac{\partial \alpha_1\rho_1 s_1 u_1 + \alpha_2\rho_2 s_2 u_2}{\partial x} = \mu(p_1 - p_2)^2\left(\frac{1}{T_1} + \frac{1}{T_2}\right) + \lambda\frac{(u_2 - u_1)^2}{Z_1 + Z_2}\left(\frac{Z_2}{T_1} + \frac{Z_1}{T_2}\right) + \frac{H(T_2 - T_1)^2}{T_1 T_2}$$

guaranteeing its thermodynamic consistency.

System (VIII.2) can also be written as,

$$\frac{\partial W}{\partial t} + A(W)\frac{\partial W}{\partial x} = 0,$$

with,

$$W = \left(s_1,\ \ s_2,\ \ \alpha_1,\ \ \rho_1,\ \ u_1,\ \ \rho_2,\ \ u_2\right)^T,$$

and,

$$A(W) = \begin{pmatrix} u_1 & 0 & 0 & 0 & 0 & 0 & 0 \\ 0 & u_2 & 0 & 0 & 0 & 0 & 0 \\ \frac{1}{\rho_1}\frac{\partial p}{\partial s_1}\Big)_{\rho_1} & 0 & u_1 & \frac{c_1^2}{\rho_1} & 0 & 0 & 0 \\ 0 & 0 & -b\rho_1 & u_1 & b\frac{\rho_1}{\alpha_1}(u_2 - u_1) & 0 & -b\rho_1\frac{\alpha_2}{\alpha_1} \\ 0 & 0 & a\alpha_1 & 0 & (au_1 - bu_2) & 0 & b\alpha_2 \\ 0 & 0 & a\rho_2\frac{\alpha_1}{\alpha_2} & 0 & a\frac{\rho_2}{\alpha_2}(u_1 - u_2) & u_2 & a\rho_2 \\ 0 & \frac{1}{\rho_2}\frac{\partial p}{\partial s_2}\Big)_{\rho_2} & 0 & 0 & 0 & \frac{c_2^2}{\rho_2} & u_2 \end{pmatrix}$$

This matrix has a nice structure. Eigenvalues are given by $\det(A - \lambda I) = 0$, which results in the following polynomial,

$$\left[(u_2 - \lambda)^2(u_1 - \lambda)^2\left((au_1 - bu_2) - \lambda\right) + (u_2 - \lambda)^2 bc_1^2\left((a - b)u_2 - \lambda\right) + (u_1 - \lambda)^2 ac_2^2\left(\lambda + (b - a)u_1\right)\right] = 0$$

When a=1, b=0 it reduces to,

$$(u_1 - \lambda)^3\left[(u_2 - \lambda)^2 - c_2^2\right] = 0$$

with the wave speeds of the first model.

When a=0, b=-1 it reduces to,

$$\left( u_2 - \lambda \right)^3 \left[ (u_1 - \lambda)^2 - c_1^2 \right] = 0$$

with the wave speeds of the symmetric model.

Therefore the flow model (VII.2) has the following wave speeds:

$\lambda_1 = u_1$, $\lambda_2 = u_1 + c_1$, $\lambda_3 = u_1 - c_1$, $\lambda_4 = u_2$, $\lambda_5 = u_2 + c_2$ and $\lambda_6 = u_2 - c_2$ . (VII.3)

However, these wave speeds are not present at any point of space. They change when the volume fraction crosses the fluidization limit ($\alpha^{\text{fluidization}}$) somewhere in the domain. In nearly all computational examples considered previously, such instance happens.

Let us mention that other guesses have been considered for parameters 'a' and 'b'. For example $a = \frac{1}{2}$, $b = -\frac{1}{2}$ yields imaginary wave speeds. Same observation appeared with $a = \alpha_2$, $b = -\alpha_1$.

For numerical computations, the first equation of System (VII.2) is expressed as,

$$\frac{\partial \alpha_1}{\partial t} + \frac{\partial \left( a \alpha_1 u_1 + b \alpha_2 u_2 \right)}{\partial x} - \left( \alpha_1 u_1 + \alpha_2 u_2 \right) \frac{\partial a}{\partial x} = 0,$$

It is solved with the hyperbolic solver of Appendix A based on the Rusanov flux. However, the wave speed estimate,

$$S = \text{Max}_k \left( |\lambda_k|_{i+1}, |\lambda_k|_i \right),$$

now involves the six eigenvalues (VII.3).

The volume fraction equation in (VII.2) being non-conservative, appropriate scheme is needed. Similar analysis as the one described in Section V is reused. Details are given in Appendix C.

Let us examine typical solutions of the general model on some test problems, as those considered previously. A shock tube test case with liquid at left and gas at right is considered, in the same conditions as the tests in Figures 5 and 9. Computed results are compared against exact solution in Figure 11.

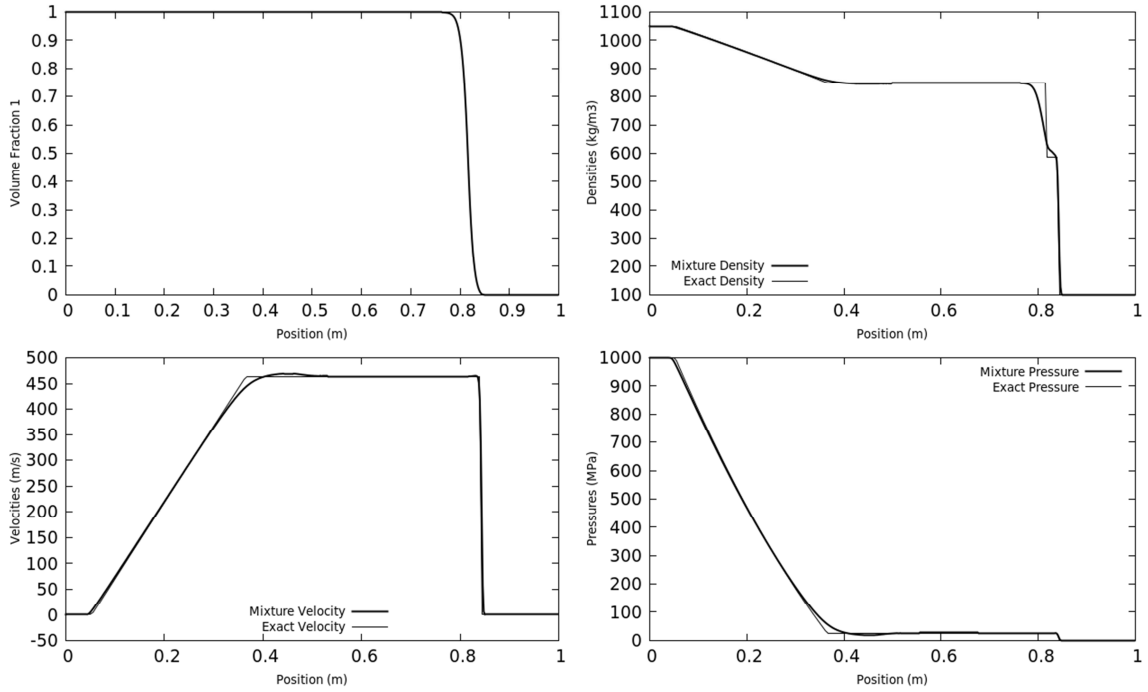


**Figure 11.** Liquid – gas shock tube test solved with the general model with stiff pressure and velocity relaxation. Computations are done with 500 cells, CFL=0.5 and van Leer limiter in the MUSCL method. Results are shown at time 250μs. The numerical solution tends to the exact one and converges quite well. Compared to the original model (Figure 5) and its symmetric variant (Figure 9) improvements are visible on both velocity and density profiles.

It is also interesting to address the Rogue test problem with the general model. Corresponding results are shown in Figure 12.

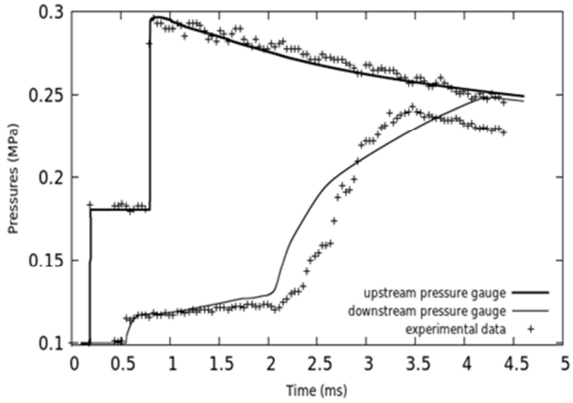


Figure 12. Computed pressure signal of the Rogue test with the general model are compared with experimental pressure records. Computations are done with 2000 cells and CFL=0.5. The various transmitted and reflected waves are correctly computed. The pressure evolution in the particle cloud has been improved but is still perfectible.

This last test shows improvements compared to Marble and BN models results:

- reflected and transmitted waves have better accuracy,
- pressure rise in the particle cloud shows better accuracy than existing models.

Possibly better agreement with experimental data could be obtained by using sophisticated drag force correlation, but this is not the scope of the present work.

Even if the BN model and the new one have the same limit model (Kapila's model) in the case of infinite pressure and velocity relaxation, the transient wave dynamics between the pure gaseous shock towards a fan of compression waves has to be well captured and seems to depend on the topology of the two-phase flow. Moreover, it can be expected that the dispersive nature of a compression wave from the BN and the new models is different.

Intergranular stress (Bdzil et al., 1999, Saurel et al., 2010) has been considered as a possible effect to improve the computations of Figure 12. These effects have been added to the present formulation and coded, but no noticeable improvement appeared.

We have also investigated the effects of the fluidization limit switch $\alpha^{fluidization}$, taken previously to 0.5. Various estimates have been tested, from 0.1 to 0.9 without noticeable changes to the results.

## VIII. Conclusion

A new two-phase hyperbolic and thermodynamically consistent model has been built and typical solutions have been computed.

It is able to compute the same flow configurations as the BN model, i.e. interfaces separating pure fluids and non-equilibrium multiphase mixtures. Its acoustic properties sound physical. Moreover, the evolution of the two-phase topology directly influences both number and speed of waves present at a given point of space. The flow dynamics expressed by the model is not only reflected through the change of drag coefficient between phases, through interfacial area evolution.

It is expected that two-phase shock waves structure be easier to analyze in the present frame. It is also expected that multidimensional solutions exhibit more differences than present one-dimensional computations, in particular regarding interface instabilities.

**Acknowledgements**. The authors are grateful to anonymous referees that helped to improve significantly the quality of the manuscript.

**References**


Abgrall, R., & Saurel, R. (2003) Discrete equations for physical and numerical compressible multiphase mixtures. Journal of Computational Physics, 186(2), 361-396

Ambroso, A., Chalons, C., & Raviart, P. A. (2012) A Godunov-type method for the seven-equation model of compressible two-phase flow. Computers & Fluids, 54, 67-91

Baer, M. R., & Nunziato, J. W. (1986) A two-phase mixture theory for the deflagration-to-detonation transition (DDT) in reactive granular materials. International Journal of Multiphase Flow, 12(6), 861-889

Bdzil, J. B., Menikoff, R., Son, S. F., Kapila, A. K., & Stewart, D. S. (1999). Two-phase modeling of deflagration-to-detonation transition in granular materials: A critical examination of modeling issues. Physics of Fluids 11(2), 378-402

Bernecker, R. R., & Price, D. (1974). Studies in the transition from deflagration to detonation in granular explosives—II. Transitional characteristics and mechanisms observed in 91/9 RDX/Wax. Combustion and Flame, 22(1), 119-129

Chinnayya, A., Daniel, E., & Saurel, R. (2004) Modelling detonation waves in heterogeneous energetic materials. Journal of Computational Physics, 196(2), 490-538

Deledicque, V., & Papalexandris, M. V. (2007) An exact Riemann solver for compressible two-phase flow models containing non-conservative products. Journal of Computational Physics 222(1), 217-245

Drew, D. A. and Passman, S. L. (2006) Theory of multicomponent fluids (Vol. 135). Springer Science & Business Media

Ergun, S. (1952) Fluid flow through packed columns. Chem. Eng. Prog., 48, 89-94

Furfaro, D., & Saurel, R. (2015) A simple HLLC-type Riemann solver for compressible non-equilibrium two-phase flows. Computers & Fluids, 111, 159-178

Ghidaglia, J. M., Kumbaro, A., & Le Coq, G. (2001) On the numerical solution to two fluid models via a cell centered finite volume method. European Journal of Mechanics-B/Fluids, 20(6), 841-867

Godunov, S. K. (2008). On approximations for overdetermined hyperbolic equations. In Hyperbolic Problems: Theory, Numerics, Applications (pp. 19-33). Springer Berlin

Houim, R. W., & Oran, E. S. (2016). A multiphase model for compressible granular–gaseous flows: formulation and initial tests. Journal of Fluid Mechanics, 789, 166-220

Kapila, A. K., Menikoff, R., Bdzil, J. B., Son, S. F., & Stewart, D. S. (2001) Two-phase modeling of deflagration-to-detonation transition in granular materials: Reduced equations. Physics of Fluids, 13(10), 3002-3024

Lhuillier, D., Chang, C. H., & Theofanous, T. G. (2013) On the quest for a hyperbolic effective-field model of disperse flows. Journal of Fluid Mechanics,731, 184-194

Marble, F.E (1963) Dynamics of a gas containing small solid particles. Combustion and Propulsion (5th AGARD Colloquium), Pergamon Press

McGrath II, T. P., Clair, J. G. S., & Balachandar, S. (2016). A compressible two-phase model for dispersed particle flows with application from dense to dilute regimes. Journal of Applied Physics, 119(17), 174903

Petitpas, F., Saurel, R., Franquet, E., & Chinnayya, A. (2009) Modelling detonation waves in condensed energetic materials: Multiphase CJ conditions and multidimensional computations. Shock Waves, 19(5), 377-401

Rusanov, V. V. E. (1962). The calculation of the interaction of non-stationary shock waves and obstacles. USSR Computational Mathematics and Mathematical Physics 1(2), 304-320

Romenski, E., & Toro, E. F. (2004). Compressible two-phase flows: two-pressure models and numerical methods. Comput. Fluid Dyn. J, 13, 403-416

Saurel, R., Daniel, E., & Loraud, J. C. (1994) Two-phase flows-Second-order schemes and boundary conditions. AIAA Journal, 32(6), 1214-1221

Saurel, R., & Abgrall, R. (1999) A multiphase Godunov method for compressible multifluid and multiphase flows. Journal of Computational Physics, 150(2), 425-467

Saurel, R., Gavrilyuk, S., & Renaud, F. (2003). A multiphase model with internal degrees of freedom: Application to shock–bubble interaction. Journal Fluid Mech, 495, 283- 321

Saurel, R., Franquet, E., Daniel, E., & Le Metayer, O. (2007). A relaxation-projection method for compressible flows. Part I: The numerical equation of state for the Euler equations. Journal of Computational Physics, 223(2), 822-845

Saurel, R., Favrie, N., Petitpas, F., Lallemand, M. H., & Gavrilyuk, S. L. (2010) Modelling dynamic and irreversible powder compaction. Journal of Fluid Mechanics, 664, 348-396

Saurel, R., Le Martelot, S., Tosello, R., & Lapebie, E. (2014) Symmetric model of compressible granular mixtures with permeable interfaces. Physics of Fluids, 26(12), 123304

Schwendeman, D. W., Wahle, C. W., & Kapila, A. K. (2006) The Riemann problem and a high-resolution

Godunov method for a model of compressible two-phase flow. Journal of Computational Physics, 212(2), 490-526
Wood, A. B. (1930). A Textbook of Sound. G. Bell and Sons Ltd., London
Zeldovich, Y.B. (1970) Gravitational instability: An approximate theory for large density perturbations. Astron. Astrophys, 5, 84–89

## Appendix A. Hyperbolic solver

We address derivation of a Godunov type method for System (IV.1-2). In the absence of source terms, it expresses in compact form as,

$$\frac{\partial U}{\partial t}+\frac{\partial F(U)}{\partial x}+H\left(U,\frac{\partial U}{\partial x}\right)=0 \qquad \text{(A.1)}$$

where,

$$U=\left(\alpha_1,\alpha_1\rho_1,\alpha_1\rho_1u_1,\alpha_1\rho_1E_1,\alpha_2\rho_2,\alpha_2\rho_2u_2,\alpha_2\rho_2E_2\right)^T,$$

$$F(U)=\begin{pmatrix}\alpha_1u_1\\ \alpha_1\rho_1u_1\\ \alpha_1\left(\rho_1u_1^2+p_1\right)\\ \alpha_1u_1\left(\rho_1E_1+p_1\right)\\ \alpha_2\rho_2u_2\\ \alpha_2\left(\rho_2u_2^2+p_2\right)\\ \alpha_2u_2\left(\rho_2E_2+p_2\right)\end{pmatrix} \text{ and } H\left(U,\frac{\partial U}{\partial x}\right)=\left(0,0,-p_I\frac{\partial\alpha_1}{\partial x},p_I\frac{\partial\alpha_1u_1}{\partial x},0,p_I\frac{\partial\alpha_1}{\partial x},-p_I\frac{\partial\alpha_1u_1}{\partial x}\right)^T.$$

The difficulty with this hyperbolic system relies in the non-conservative term $H\left(U,\frac{\partial U}{\partial x}\right)$.

For the sake of simplicity the Rusanov (1962) approximate Riemann solver is considered. It uses the following estimate for the right facing wave, at a given cell boundary separating cells i and i+1:

$$S=\mathrm{Max}_k\left(\left|\lambda_k\right|_{i+1},\left|\lambda_k\right|_i\right).$$

At a given cell boundary separating left (L) and right (R) states, the approximate flux reads,

$$F^*=\frac{1}{2}\left[F_R+F_L-S\left(U_R-U_L\right)\right] \qquad \text{(A.2)}$$

The Godunov scheme for System (A.1) necessarily reads,

$$U_i^{n+1}=U_i^n-\frac{\Delta t}{\Delta x}\left(F_{i+1/2}^*-F_{i-1/2}^*\right)+\Delta tH_i \qquad \text{(A.3)}$$

where $H_i$ is the numerical approximation of $H\left(U,\frac{\partial U}{\partial x}\right)$, to be determined.

To determine $H_i$, we follow Saurel and Abgrall (1999) where a flow in uniform mechanical equilibrium is considered:

$$u_{1,i-1}=u_{1,i}=u_{1,i+1}=u_{2,i-1}=u_{2,i}=u_{2,i+1}=u>0$$

$$p_{1,i-1}=p_{1,i}=p_{1,i+1}=p_{2,i-1}=p_{2,i}=p_{2,i+1}=p$$

Inserting the Rusanov flux (A.2) in the Godunov method (A.3) for the mass equation of the first phase, the following result is obtained:

$$(\alpha_1\rho_1)_i^{n+1}=(\alpha_1\rho_1)_i^n-\frac{u\Delta t}{2\Delta x}\left[(\alpha_1\rho_1)_{i+1}-(\alpha_1\rho_1)_{i-1}\right]+\frac{S\Delta t}{2\Delta x}\left[(\alpha_1\rho_1)_{i+1}-2(\alpha_1\rho_1)_i+(\alpha_1\rho_1)_i\right] \qquad \text{(A.4)}$$

The same procedure is done for the momentum equation of the same phase:

$$(\alpha_1\rho_1u_1)_i^{n+1} = u\overbrace{\left[(\alpha_1\rho_1)_i^n - \frac{u\Delta t}{2\Delta x}\left[(\alpha_1\rho_1)_{i+1} - (\alpha_1\rho_1)_{i-1}\right] + \frac{S\Delta t}{2\Delta x}\left[(\alpha_1\rho_1)_{i+1} - 2(\alpha_1\rho_1)_i + (\alpha_1\rho_1)_i\right]\right]}^{(\alpha_1\rho_1)_i^{n+1}}$$

$$-\frac{\Delta t}{2\Delta x}p\left[\alpha_{1,i+1} - \alpha_{1,i-1}\right] + H_{i,u}$$

In order that $u_{1,i}^{n+1} = u$, the non-conservative term $H_{i,u}$ must be approximated as,

$$H_{i,u} = p_i^n\frac{\alpha^*_{1,i+1/2} - \alpha^*_{1,i-1/2}}{\Delta x} \text{ with } \alpha^*_{1,i+\frac{1}{2}} = \frac{\alpha_{1,i+1} + \alpha_{1,i}}{2}. \quad \text{(A.5)}$$

Considering the balance energy equation of the same phase the following discrete approximation is obtained:

$$\left(\alpha_1\rho_1E_1\right)_i^{n+1} = \left(\alpha_1\rho_1E_1\right)_i^n - \frac{\Delta t}{2\Delta x}\left[\left(\alpha_1u_1\left(\rho_1E_1 + p_1\right)\right)_{i+1} - \left(\alpha_1u_1\left(\rho_1E_1 + p_1\right)\right)_{i-1}\right]$$

$$+\frac{\Delta tS}{2\Delta x}\left(\left(\alpha_1\rho_1E_1\right)_{i+1} - 2\left(\alpha_1\rho_1E_1\right)_i + \left(\alpha_1\rho_1E_1\right)_{i-1}\right) + p_i^n\frac{\Delta t}{\Delta x}\left[\left(\alpha_1u_1\right)^*_{i+1/2} - \left(\alpha_1u_1\right)^*_{i-1/2}\right]$$

The same analysis as before to maintain mechanical equilibrium provides the following guess:

$$H_{i,u} = p_i^n\frac{\left(\alpha_1u_1\right)^*_{i+1/2} - \left(\alpha_1u_1\right)^*_{i-1/2}}{\Delta x} \text{ with } \left(\alpha_1u_1\right)^*_{i+1/2} = \frac{(\alpha_1u_1)_{i+1} + (\alpha_1u_1)_i}{2} \quad \text{(A.6)}$$

The flow solver thus consists in (A.3) with (A.2), (A.5) and (A.6).

## Appendix B. Stiff pressure and velocity relaxation solvers

### a) Stiff pressure relaxation

The system to consider for phase 1 during pressure relaxation is the following:

$$\begin{cases} \dfrac{\partial\alpha_1}{\partial t} = \mu\left(p_1 - p_2\right) \\ \dfrac{\partial\alpha_1\rho_1}{\partial t} = 0 \\ \dfrac{\partial\alpha_1\rho_1u_1}{\partial t} = 0 \\ \dfrac{\partial\alpha_1\rho_1e_1}{\partial t} = -\mu p_I\left(p_1 - p_2\right) \end{cases}$$

Combining the internal energy equation of phase 1 with the corresponding volume fraction equation results in,

$$\frac{\partial e_1}{\partial t} = -p_I\frac{\partial v_1}{\partial t}$$

where v is the specific volume of the considered phase.

Considering the relaxed pressure as a constant during time integration, it becomes (this assumption has been analyzed in Saurel et al., 2007),

$$e_1^* - e_1^0 = -p^*\left(v_1^* - v_1^0\right) \quad \text{(B.1)}$$

The stiffened gas equation of state (alternatively given by Equation V.1) is inserted (any other convex EOS can be considered as well),

$$e_k\left(p_k, v_k\right) = \frac{p_k + \gamma_kp_{k\infty}}{\gamma_k - 1}v_k.$$

Consequently (B.1) becomes,

$$\frac{p^* + \gamma_1 p_{1\infty}}{\gamma_1 - 1} v_1^* - \frac{p_1^0 + \gamma_1 p_{1\infty}}{\gamma_1 - 1} v_1^0 = -p^* \left( v_1^* - v_1^0 \right)$$

I.e.,

$$\alpha_1^* = \alpha_1^0 + \frac{\alpha_1^0}{\gamma_1} \left( \frac{p_1^0 + p_{1\infty}}{p^* + p_{1\infty}} - 1 \right) \tag{B.2}$$

Same result is obtained for the second phase,

$$\alpha_2^* = \alpha_2^0 + \frac{\alpha_2^0}{\gamma_2} \left( \frac{p_2^0 + p_{2\infty}}{p^* + p_{2\infty}} - 1 \right)$$

The saturation constraint $\sum_{k=1}^{N} \alpha_1^* = 1$ is then considered resulting in the following root for the equilibrium pressure:

$$p^* = \frac{1}{2}\left( A_1 + A_2 - p_{1\infty} - p_{2\infty} \right) + \sqrt{\frac{1}{4}\left( A_2 - A_1 + p_{1\infty} - p_{2\infty} \right)^2 + A_1 A_2} \tag{B.3}$$

where, $A_1 = \dfrac{\dfrac{\alpha_1^0}{\gamma_1}\left( p_1^0 + p_{1\infty} \right)}{\dfrac{\alpha_1^0}{\gamma_1} + \dfrac{\alpha_2^0}{\gamma_2}}$ and $A_2 = \dfrac{\dfrac{\alpha_2^0}{\gamma_2}\left( p_2^0 + p_{2\infty} \right)}{\dfrac{\alpha_1^0}{\gamma_1} + \dfrac{\alpha_2^0}{\gamma_2}}$.

Once the relaxed pressure is determined with (B.3) the volume fractions at equilibrium are determined with (B.2).

**b) Stiff velocities relaxation**

During stiff velocity relaxation, the subsystem to consider reads,

$$\frac{\partial \alpha_1 \rho_1}{\partial t} = 0$$

$$\frac{\partial \alpha_1 \rho_1 u_1}{\partial t} = \lambda (u_2 - u_1)$$

$$\frac{\partial \alpha_1 \rho_1 e_1}{\partial t} = \lambda (u_2 - u_1)(u_I - u_1)$$

$$\frac{\partial \alpha_2 \rho_2}{\partial t} = 0$$

$$\frac{\partial \alpha_1 \rho_1 u_1 + \alpha_2 \rho_2 u_2}{\partial t} = 0$$

$$\frac{\partial \alpha_1 \rho_1 E_1 + \alpha_2 \rho_2 E_2}{\partial t} = 0$$

where $u_I$ is defined by (IV.3).

As $\lambda \to +\infty$ both velocities relax to the equilibrium one given by the mixture momentum equation,

$$u^* = \frac{\alpha_1 \rho_1 u_1 + \alpha_2 \rho_2 u_2}{\alpha_1 \rho_1 + \alpha_2 \rho_2}$$

The velocities of the phases are then reset to this value.

The internal energy of the phases are corrected as,

$$e_k = e_k^0 + \left( u_I - u_k \right)^0 (u^* - u_k^0) \text{ with } u_I = \frac{Z_1 u_1 + Z_2 u_2}{Z_1 + Z_2} .$$

Such velocity relaxation modifies both kinetic and internal energies. Pressure relaxation is thus needed after velocity relaxation.

**Appendix C. Derivation of the volume fraction numerical scheme for System (VII.2)**

The volume fraction equation,

$$\frac{\partial \alpha_1}{\partial t}+\frac{\partial\left(a\alpha_1 u_1+b\alpha_2 u_2\right)}{\partial x}-\left(\alpha_1 u_1+\alpha_2 u_2\right)\frac{\partial a}{\partial x}=0,$$

must have a discretization compatible with the mass equation of the same system,

$$\frac{\partial(\alpha\rho)_1}{\partial t}+\frac{\partial(\alpha\rho u)_1}{\partial x}=0.$$

In uniform velocity flows conditions, using the Rusanov flux (A.2) in the Godunov method (A.3), the discrete mass equation results in (A.4).

The same is done for the volume fraction equation,

$$(\alpha_1)_i^{n+1}=(\alpha_1)_i^n-\frac{u\Delta t}{2\Delta x}\left[(a\alpha_1+b\alpha_2)_{i+1}-(a\alpha_1+b\alpha_2)_{i-1}\right]+\frac{S\Delta t}{2\Delta x}\left[(\alpha_1)_{i+1}-2(\alpha_1)_i+(\alpha_1)_{i-1}\right]+u\Delta t\frac{\Delta a}{\Delta x} \quad \text{(C.1)}$$

where $\frac{\Delta a}{\Delta x}$ is the numerical approximation of $\frac{\partial a}{\partial x}=0$, to be determined.

Rearranging (C.1) with $b=a-1$ and $\alpha_2=1-\alpha_1$ the discrete volume fraction equation becomes,

$$(\alpha_1)_i^{n+1}=(\alpha_1)_i^n-\frac{u\Delta t}{2\Delta x}\left[\alpha_{1i+1}-\alpha_{1i-1}\right]-\frac{u\Delta t}{2\Delta x}\left[a_{i+1}-a_{i-1}\right]+\frac{S\Delta t}{2\Delta x}\left[(\alpha_1)_{i+1}-2(\alpha_1)_i+(\alpha_1)_{i-1}\right]+u\Delta t\frac{\Delta a}{\Delta x} \quad \text{(C.2)}$$

Let us now consider the particular case of uniform density field: $\rho_{1,i}^{\ n}=\rho_{1,i+1}^{\ n}=\rho_{1,i-1}^{\ n}$.

Both velocity and density being uniform, the density at the next time step must be invariant: $\rho_{1,i}^{\ n+1}=\rho_{1,i}^{\ n}$.

In this context, the mass equation becomes,

$$(\alpha_1\rho_1)_i^{n+1}=\rho_1\left\{(\alpha_1)_i^n-\frac{u\Delta t}{2\Delta x}\left[(\alpha_1)_{i+1}-(\alpha_1)_{i-1}\right]+\frac{S\Delta t}{2\Delta x}\left[(\alpha_1)_{i+1}-2(\alpha_1)_i+(\alpha_1)_{i-1}\right]\right\} \quad \text{(C.3)}$$

In order that (C.2) and (C.3) be compatible it is necessary that,

$$-\frac{u\Delta t}{2\Delta x}\left[a_{i+1}-a_{i-1}\right]+u\Delta t\frac{\Delta a}{\Delta x}=0$$

Therefore,

$$\frac{\Delta a}{\Delta x}=\frac{a_{i+1}-a_{i-1}}{2\Delta x} \quad \text{(C.4)}$$

or,

$$\frac{\Delta a}{\Delta x}=\frac{a_{i+1/2}^*-a_{i-1/2}^*}{\Delta x},$$

with $a_{i+1/2}^*=\frac{a_{i+1}^n+a_i^n}{2}$.

Consequently the volume fraction scheme reads,

$$\alpha_{1,i}^{n+1}=\alpha_{1,i}^n-\frac{\Delta t}{\Delta x}\left(F_{\alpha i+1/2}^*-F_{\alpha i-1/2}^*\right)+\left(\alpha_1 u_1+\alpha_2 u_2\right)_i^n\,\Delta t\frac{\Delta a}{\Delta x} \quad \text{(C.5)}$$

with ,

$$F_{\alpha i+1/2}^*=\frac{1}{2}\left[\left(a\alpha_1 u_1+b\alpha_2 u_2\right)_{i+1}^n+\left(a\alpha_1 u_1+b\alpha_2 u_2\right)_i^n-S\left(\alpha_{1,i+1}^{\ n}-\alpha_{1,i}^{\ n}\right)\right].$$